

# Beam size and Emittance measurement at the EXT line of ATF2

**A. Faus-Golfe**

**on behalf of mOTR team:**

A. Faus-Golfe, J. Alabau, C. Blanch, J. Resta Lopez J. Navarro Faus

**IFIC Valencia**

D. McCormick, G. White, J. Cruz, M. Woodley, E. Marin

**SLAC**

with

**KEK support**

# Outline

---

- Introduction and Objectives
- Technical Description and Capabilities
  - Hardware and Software
  - First measurements
  - Beam size and Emittance measurements
  - Other applications: Coupling correction, Beta matching, Energy spread measurement
- Emittance reconstruction analysis
- Lessons learned and implications to ILC
- Conclusions

# Introduction and Objectives

---

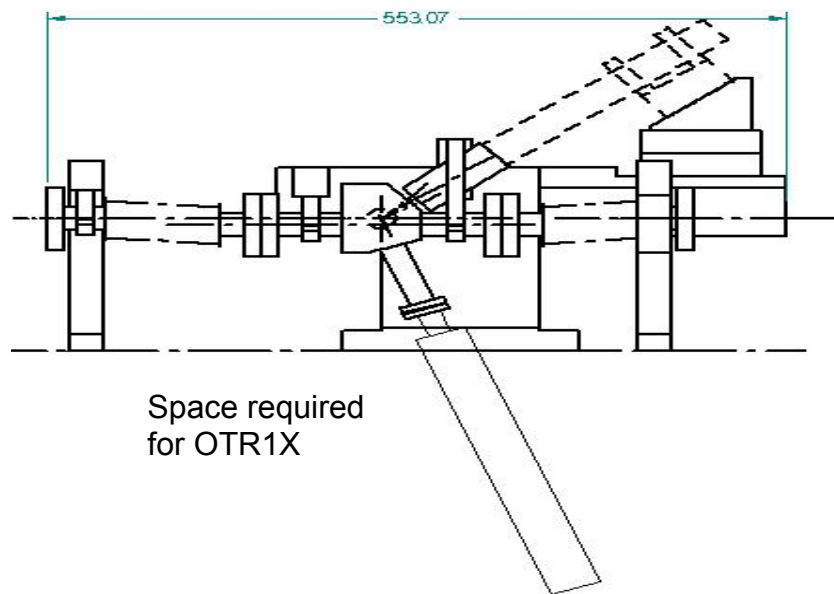
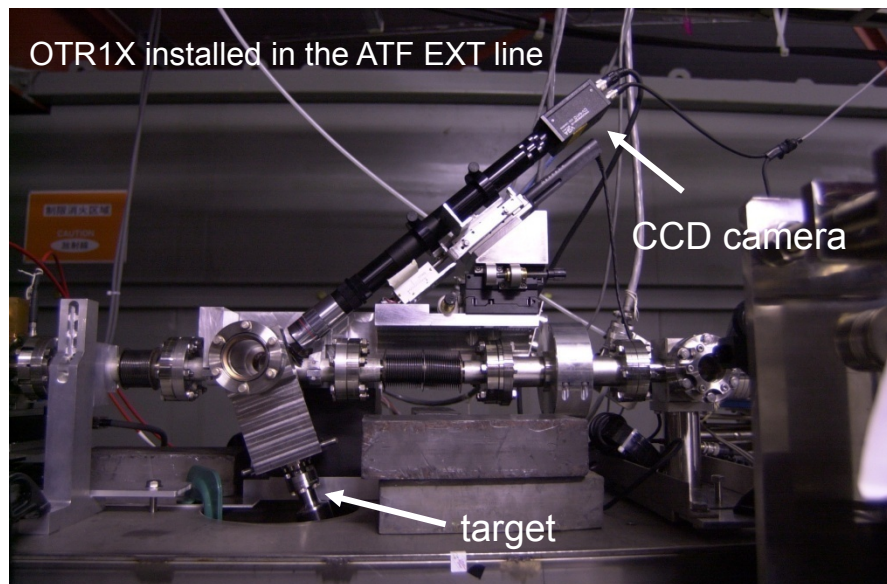
- The multi-OTR system is made of **4 OTRs** installed in the zero-dispersion part of ATF2 EXT line
- The objective of this project is the **fast measurement of the emittance** (single shot for beam size, 1min for emittance) with:
  - high statistics
  - **2 $\mu$ m** resolution
  - **$2 \times 10^{10}$  single bunch** and  **$2 \times 10^{11}$  for 20 multi-bunched** beam (2.8 ns spacing)
- The design is based on OTR1X at ATF EXT line (**5 $\mu$ m resolution with  $2 \times 10^{10}$** ) including improved features (compactness, calibration setup, demagnifier system..)
- The system **is installed near WS** for comparison and confirmation of OTR as a beam emittance diagnostic device



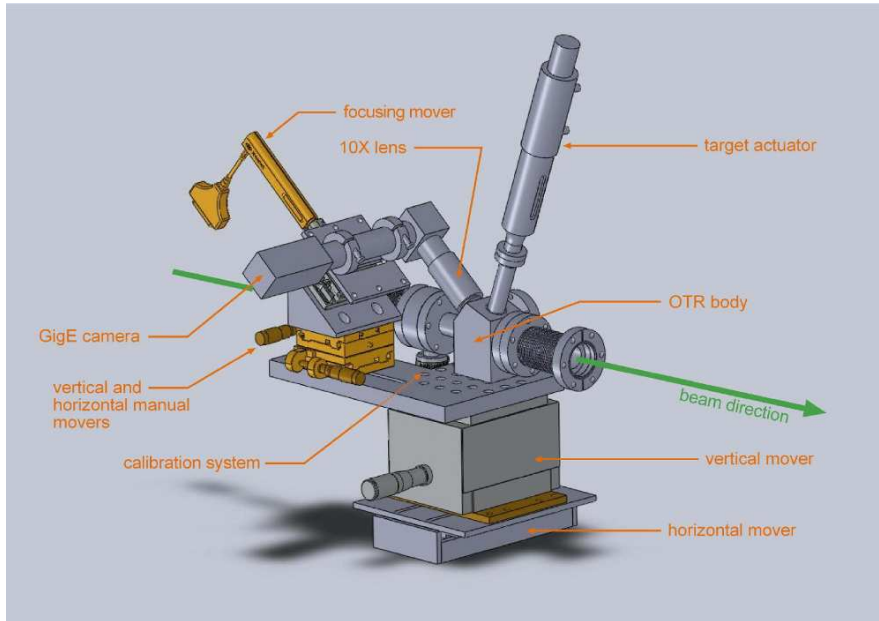
# Timeline

---

- **Proposal to ATF2 collaboration** June 2009
- **Design and Construction** Fall 2009
- **Calibration at IFIC and SLAC labs** February 2010
- **Installation in the ATF2 EXT line** April-May 2010
- **First Test with beam** June 2010
- **Test, Software Developments for beam size and emittance reconstruction and implementation in ATF2 control system** Fall 2010
- **New targets, Calibration system and Camera protection system** November 2010
- **Software Developments, Calibration and First Beam Measurements** Nov-Dec 2010
- **New LAN Control system** February 2011
- **Systematic Measurements I (before Tohoku earthquake)** January-March 2011
- **Design and Construction of a Demagnifier system** January-April 2011
- **Installation of the Demagnifier system** August 2011
- **Development of Coupling correction software algorithms** from September 2011
- **Systematic Measurements II (after Tohoku earthquake)** Nov 2011- Dec 2012
- **Proposal of new Target holders and Optical system** September 2012
- **Design and Construction of new Target holders** February-December 2012
- **New Target holder Installation** February 2013
- **Systematic measurements III** from March 2013



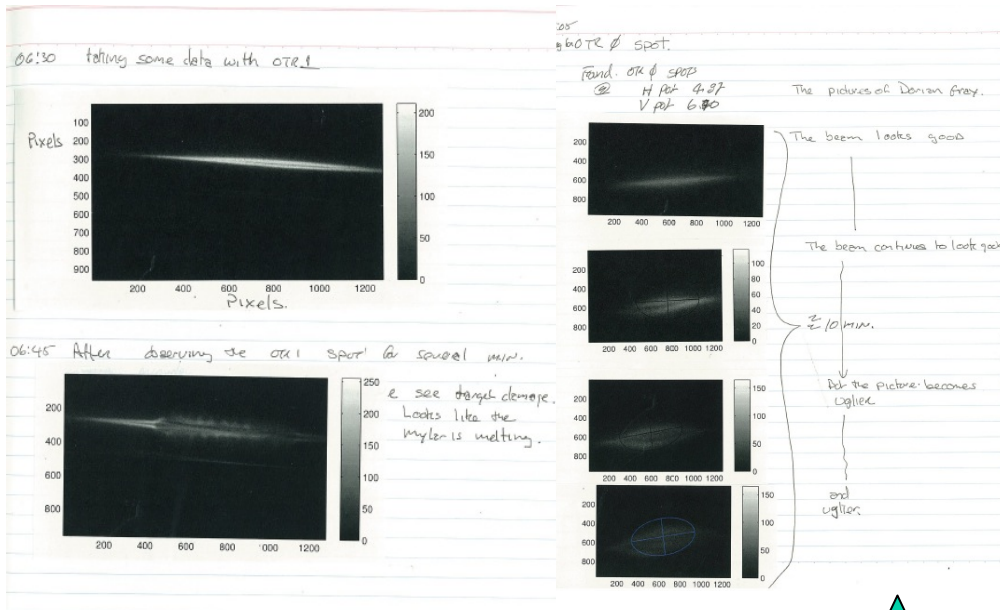
- The OTR1X was an **evolved design** rather than a **optimized one**. New parts were added to the existing OTR to add functionality, instead of making a new design. As a result the OTR1X was a patchwork of parts, taking up **a lot of beam line space**.
- The OTR **targets** were rather **thick**, about 0.5 mm of copper, beryllium or glassy carbon. This caused radiation darkening of the glass lens and camera damage.
- The camera **CCD** was **not parallel** to the **target**. This meant that the beam spot was in focus on only a small portion of the target. If the **beam moved**, the **image** had to be **refocused**.



**New OTRs have same controls and motion capabilities** as OTR1X with the following improvements:

- **Target actuator** relocated to the **top** (no interference with the girder) and smaller design, giving greater flexibility in the OTR placement
- **Thinner target** that **reduces lens radiation darkening**

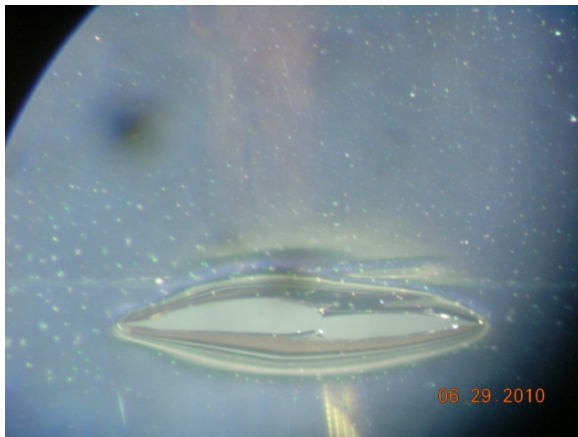
- The extreme **thinness** of the **aluminium target** reduces the **power deposition** in the aluminium and coupled to larger beam spot sizes should **eliminate target damage** problems.
- **CCD** camera “**parallel**” to the **target**. This puts the entire target into focus and **reduces** the need to **adjust focus** during normal operation giving greater depth of field.
- 12 bit **camera** for **more dynamic range** with **smaller pixel size** (3.75x3.75um) for more resolution (1280x960 pixels) with CCD sensor 1/3”
- **Calibration system** when there is no beam includes small lamp



- Exercise and **calibration** of vertical and horizontal **movers** and read-back **potentiometers**

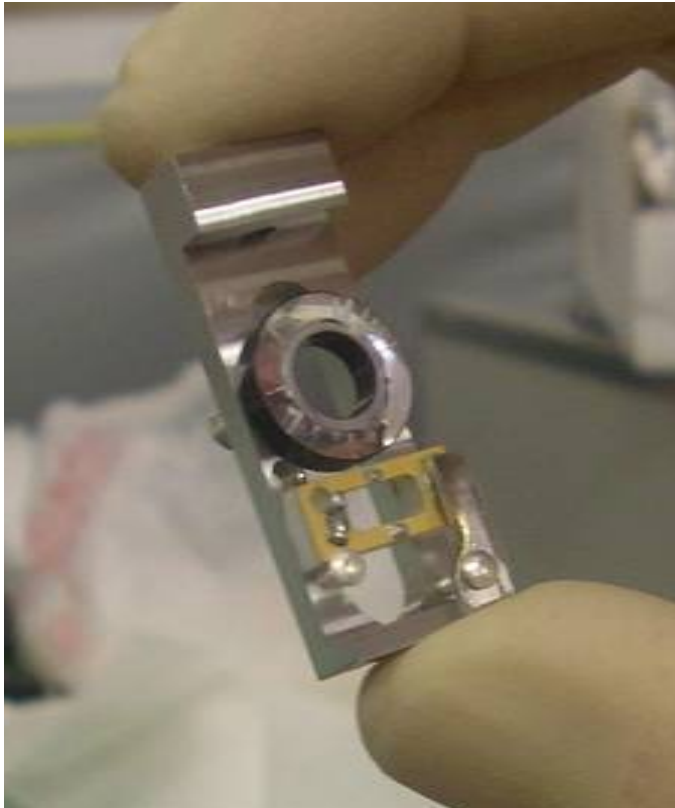
- Tests of 4 OTRs during beam time: beam seen but 3 **targets** (nitrocellulose coated aluminum) were **damaged** ( $4 \times 10^9$  e<sup>-</sup> per pulse)

- **CCD Cameras** suffer from **radiation**, some pixel are dead



Damaged target





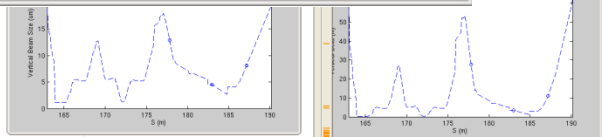
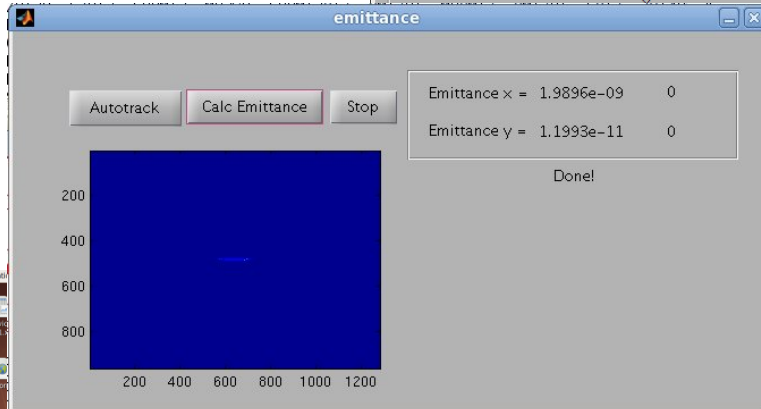
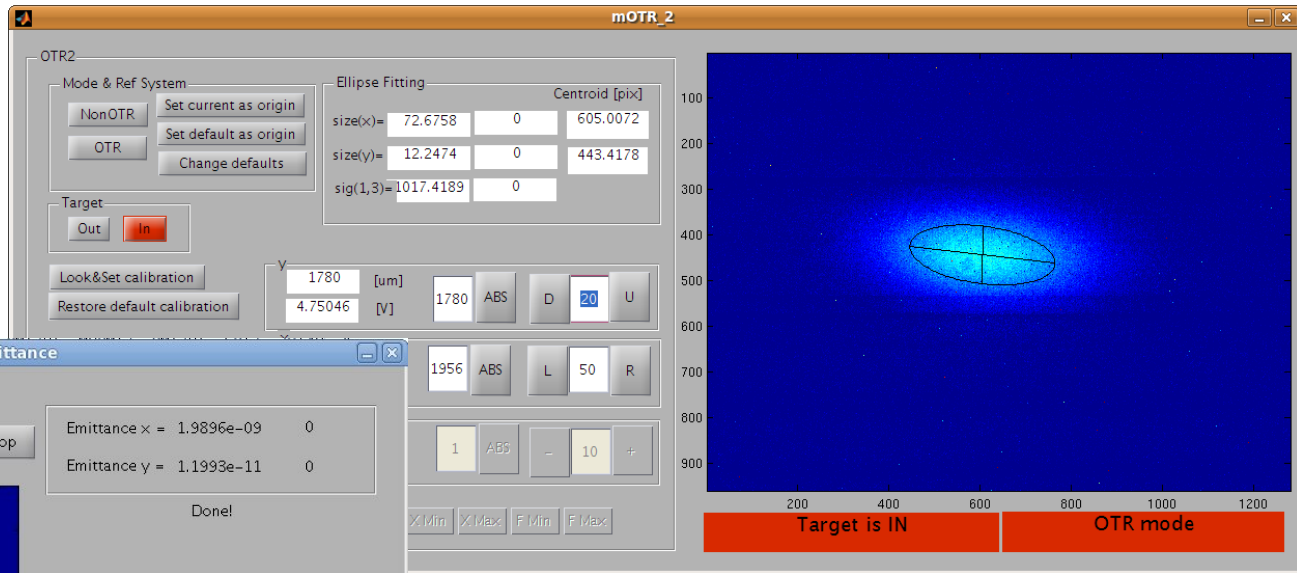
New targets could **stand the beam currents** for several minutes without being damaged



Two **new targets** were installed, two made with **aluminium (2um)** and two with **aluminized kapton (3-5um with 1200 Amstrongs Al coating)**. Besides, together with all them, the **wire targets, made with 4 wire (10um tungsten)**, one horizontal, one vertical and two tilted were installed.

# Technical Description SW I

November 2010: First calibration of vertical scale and first software test



First **GUI tests** and some **initial calibrations** using IPBMS were made



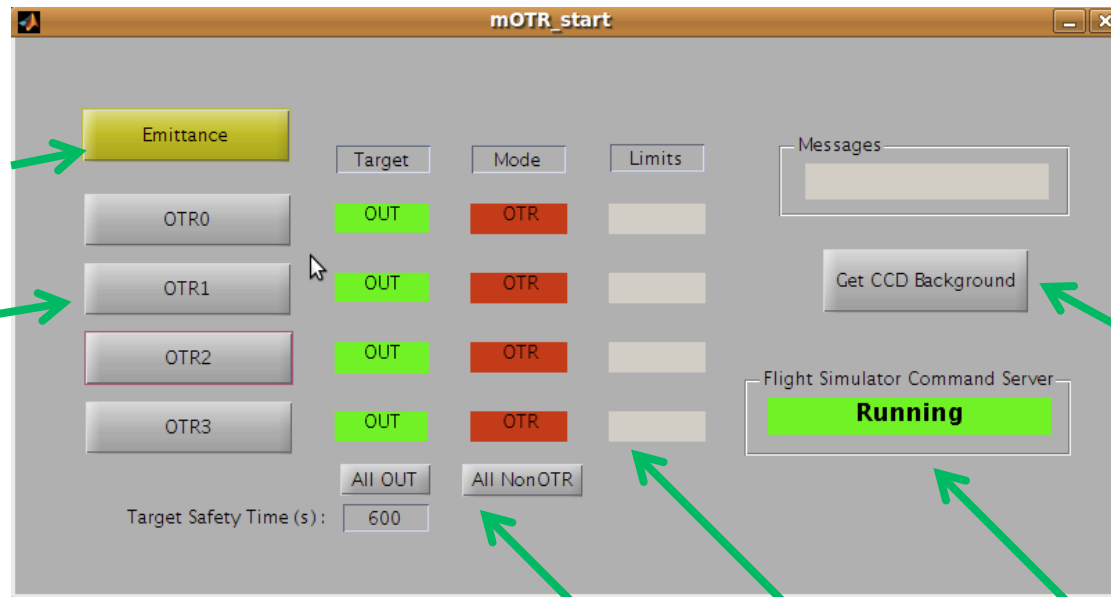
3-4 April

ATF2 Technical Review

10

- **OTR software** is an standalone compiled executable from **Matlab**.
- Some functions like **emittance calculation** or beam finder need the Flight Simulator running.
- OTR status reported and displayed on global **ATF alarm panel** showing **OTR actuator status**.
- All useful **data are stored in EPICS** Process Variables and archived in the EPICS archival system.

### Main start panel



Emittance calculation  
(next slides)

Single OTR panel  
(next slides)

Get CCD Background

Flight simulator Status

Some machine status

Some protection controls

## Single OTR panel

The screenshot shows the mOTR\_2 software interface. On the left, several green arrows point to specific sections: 'Working mode & Reference system' (pointing to Mode & Ref System), 'Target control' (pointing to Target buttons), 'Calibrations' (pointing to Calibration Settings), 'Beam finder' (pointing to Beam Finder buttons), and 'CCD Gain' (pointing to Gain and Max ADC fields). At the bottom left, an arrow points to 'Position & movement of the movers' (pointing to the Beam Presence Cut section). On the right, a large plot area shows a 2D beam profile with a red ellipse fit. A green arrow points to the 'number of measurements' (Ave: 10) above the plot. Another green arrow points to the 'Machine status' bar at the bottom of the plot area, which shows 'Target is IN' and 'OTR mode'. A third green arrow points to the 'Limit switches status' bar below the plot area, which shows '1' and a red bar. A fourth green arrow points to the 'Ellipse fitting and analysis' table in the center of the interface. A fifth green arrow points to the 'CCD image and beam fitting' area, which includes the 2D plot and the ellipse fit.

Working mode & Reference system

Target control

Calibrations

Beam finder

CCD Gain

Position & movement of the movers

number of measurements

Machine status

Limit switches status

Ellipse fitting and analysis

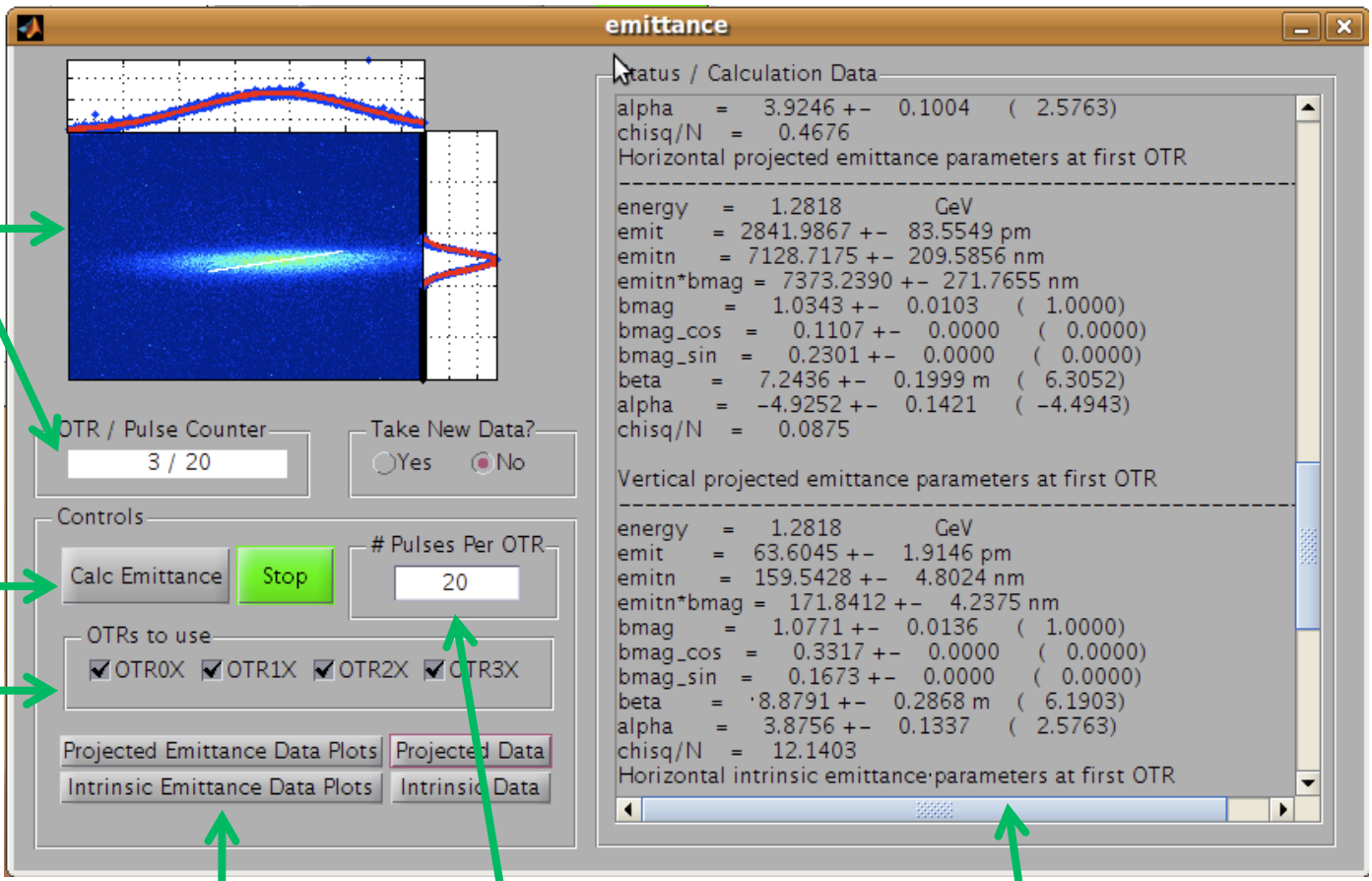
CCD image and beam fitting

|       |          |         |
|-------|----------|---------|
| sx    | 72.0418  | 0.37007 |
| sy    | 21.8911  | 0.21814 |
| sxy   | 943.6329 | 14.269  |
| X     | 294.8829 | 6.914   |
| Y     | 184.1296 | 6.39    |
| projX | 97.7062  | 0.73738 |
| projY | 26.3838  | 0.38082 |

|   |   |        |     |
|---|---|--------|-----|
| N | 3 | % Peak | 0.2 |
|---|---|--------|-----|

|   |      |
|---|------|
| 1 | 1743 |
|---|------|

### Emittance panel



Current OTR info

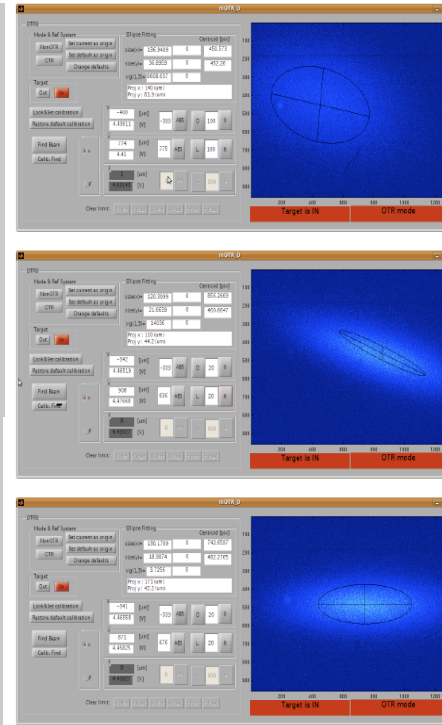
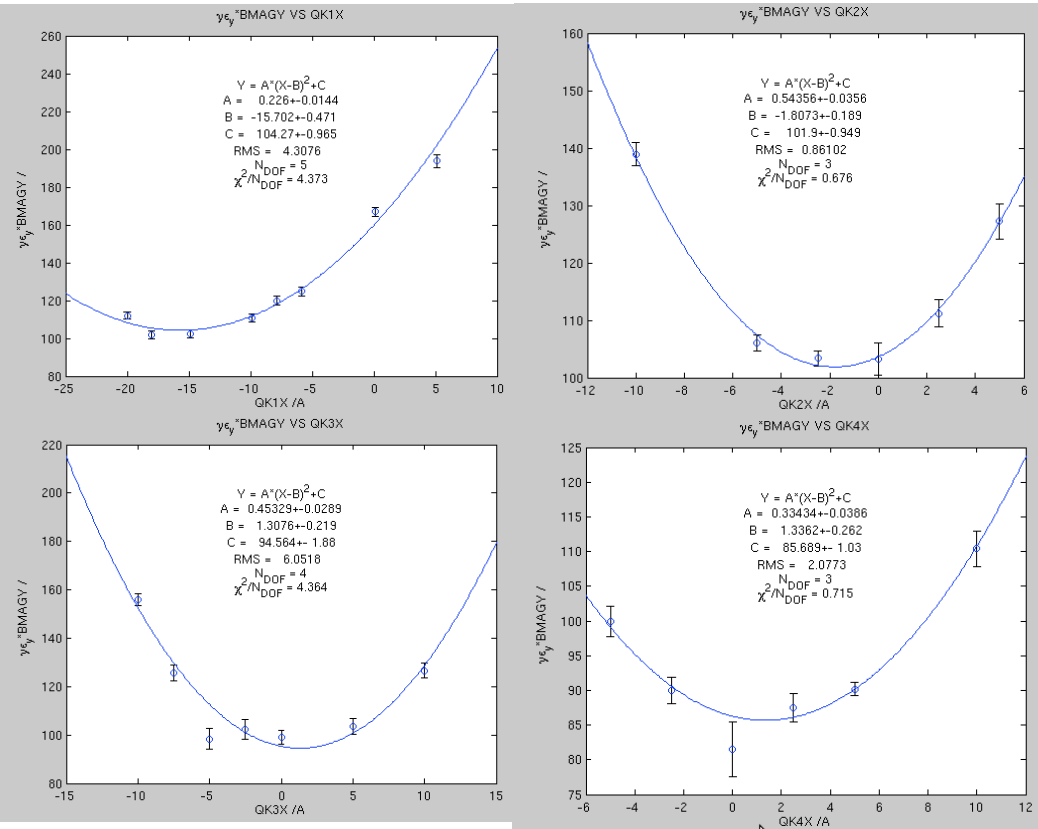
Start/stop emittance procedure

Number of OTR to be used

Data analysis and plots

number of measurements per OTR

Calculation data

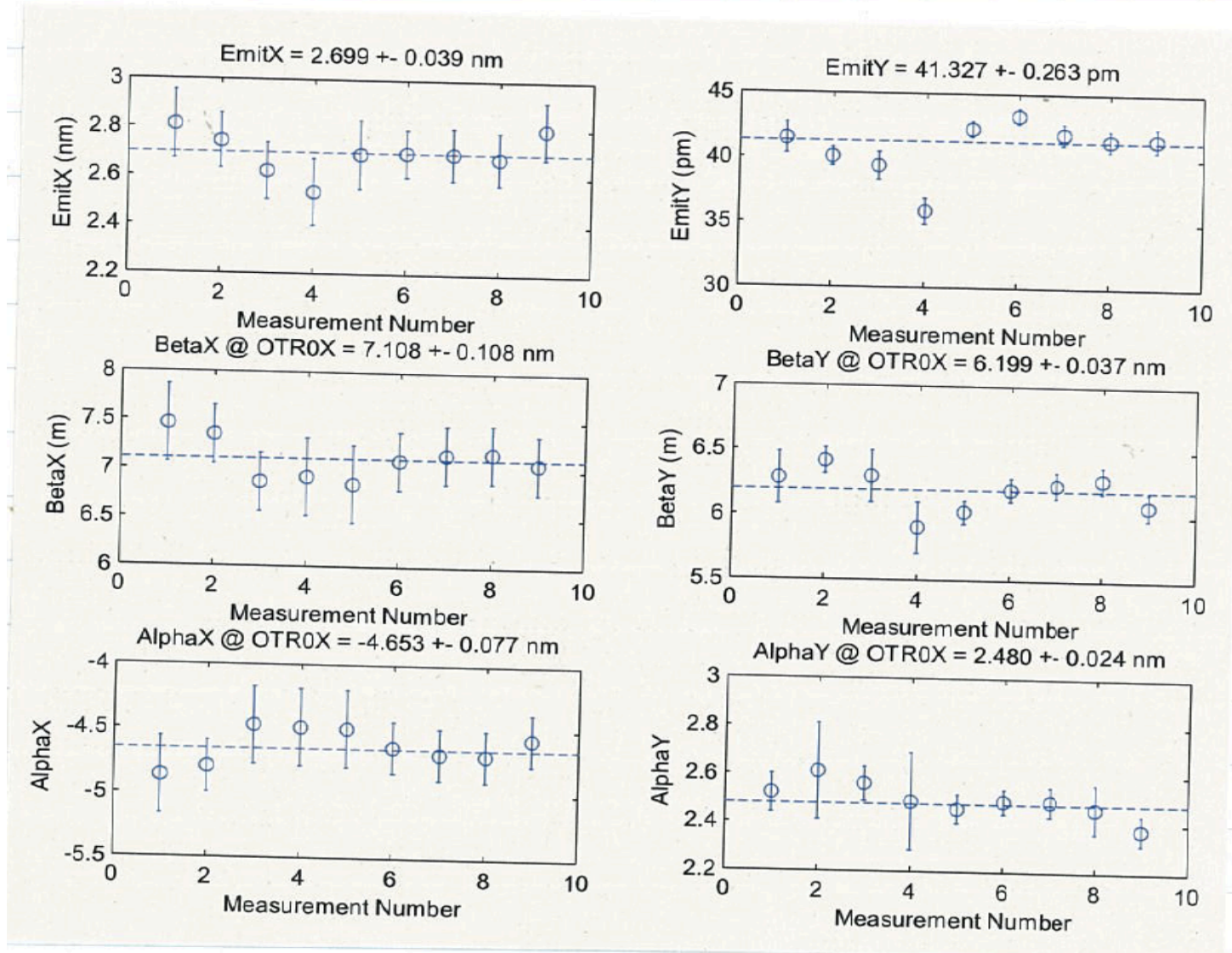


OTR0X before corrections

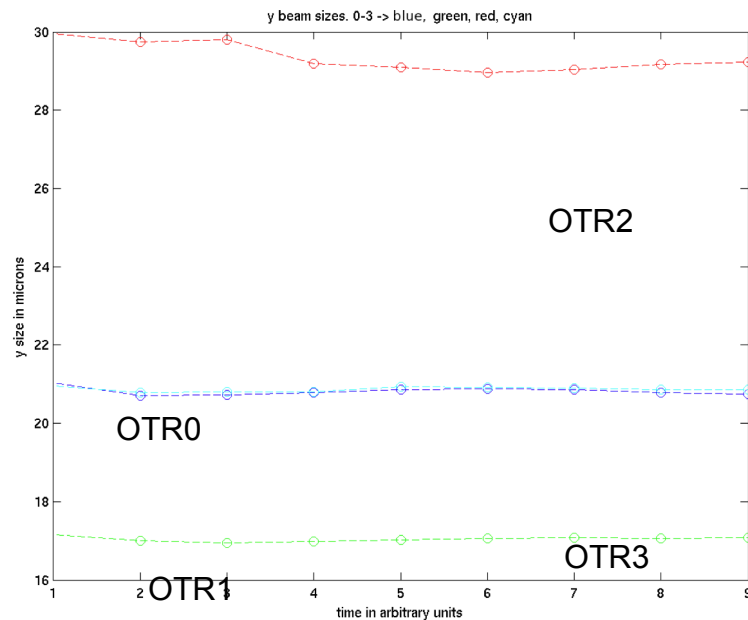
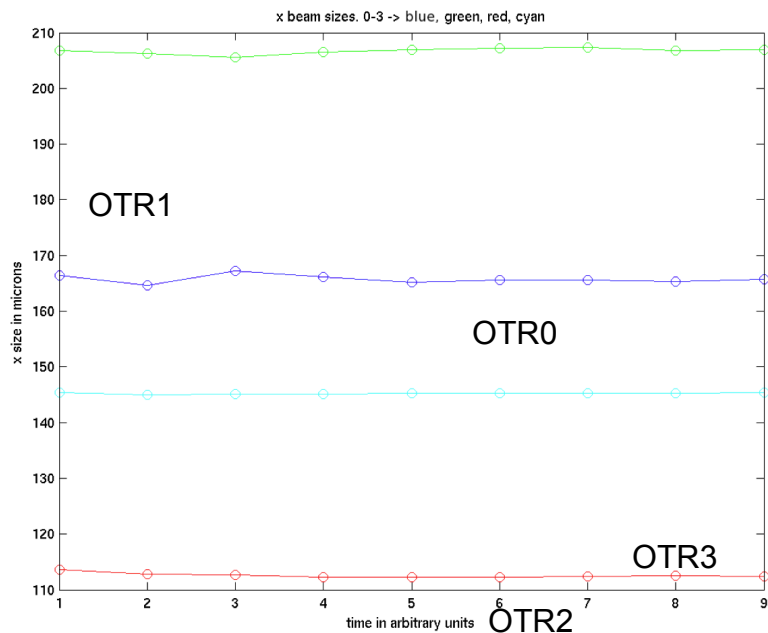
OTR0X after dispersion correction

OTR0X after coupling correction

**Coupling correction in the EXT line was achieved by scanning each of the 4 EXT skew quads. For each scan the quantity:  $\gamma\epsilon_y \cdot \text{BMAGY}$  is plotted and the optimal value of the skew quad comes from the parabolic fit.**



**Calibrations and alignments** were made during the first part of the 2011 run period before starting a **systematic measurement campaign**

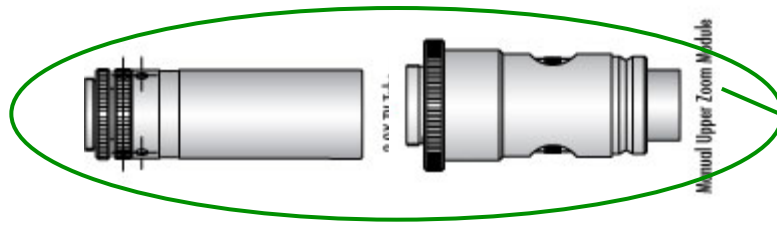




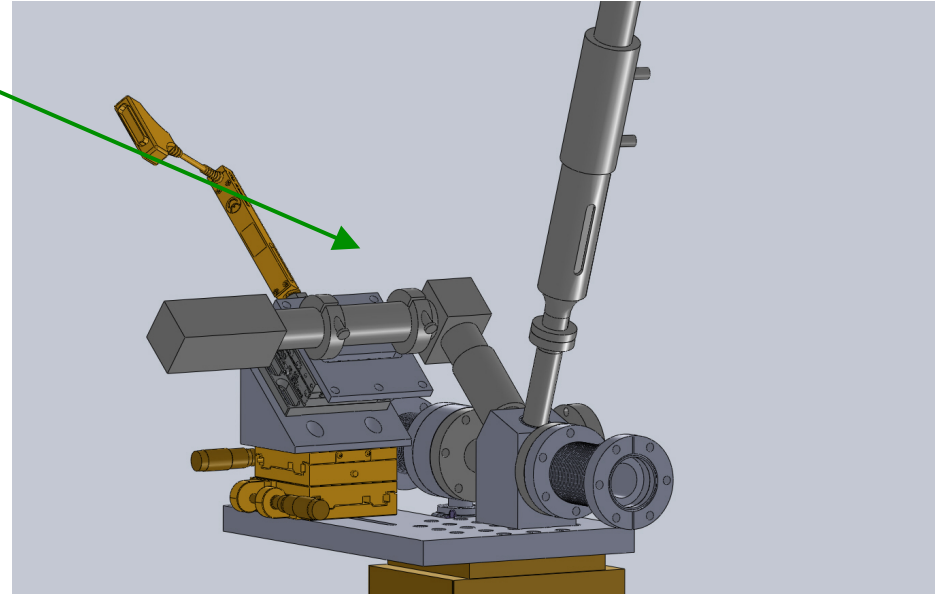
# Technical Description HW II

January/August 2011: Demagnifier system Design, Construction

A **demagnifier** system to speed up the **beam finding** and to measure **horizontal** size when **beam** is **large** in x was designed



## NEW MOTORIZED ZOOM SYSTEM

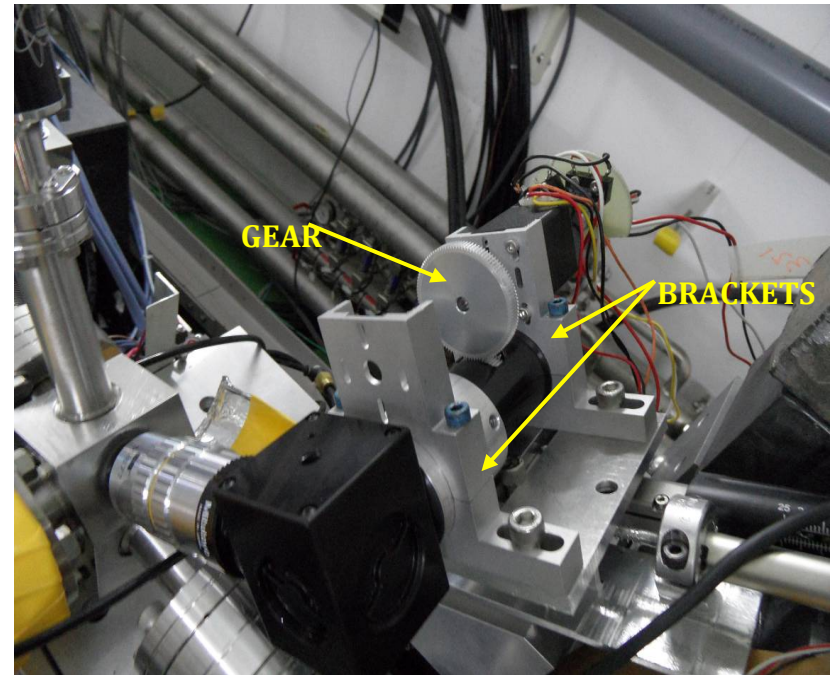
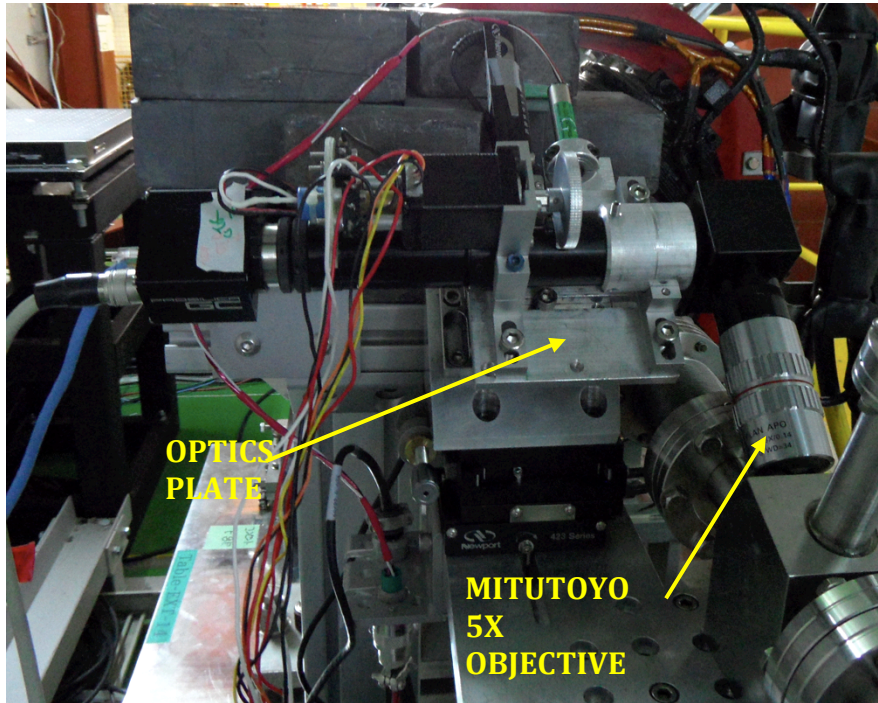


- 2.0X TV Tube: Position the camera at the proper distance from the zoom
- Upper zoom module: Contains the core zoom system.
- Motorized by an independent step motor

**Pros:** - Lighter and less bulky than the switchable lens system, easier installation  
- Better lenses performance  
- Allows beam finding and measurements in 2 different magnification (5X and 10X) by calibrating the system in both states.

**Cons:** - Larger number of optical elements and therefore a greater light absorption, meaning slightly dimmer spots.

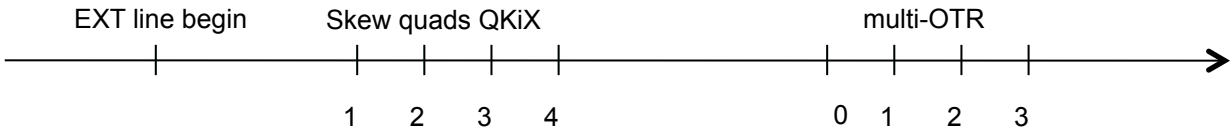
The **demagnifier zoom** system was **installed** in August 2011



The zoom system was installed in the same place where before an empty optic tube was located, between the 45° mirror and the CCD camera.

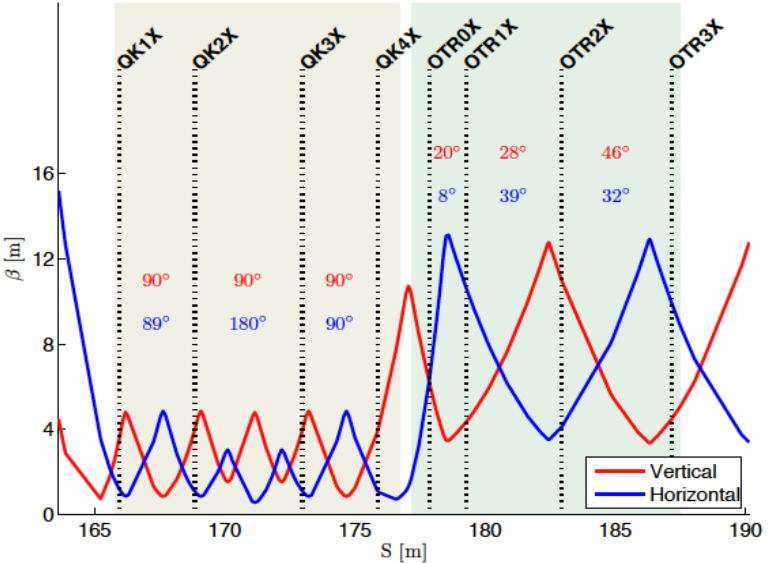
The Mitutoyo 10X lenses were substituted by a 5X lenses allowing the system to operate in a range of **magnification** between **3.6X** and **25X**

## Response Matrix method

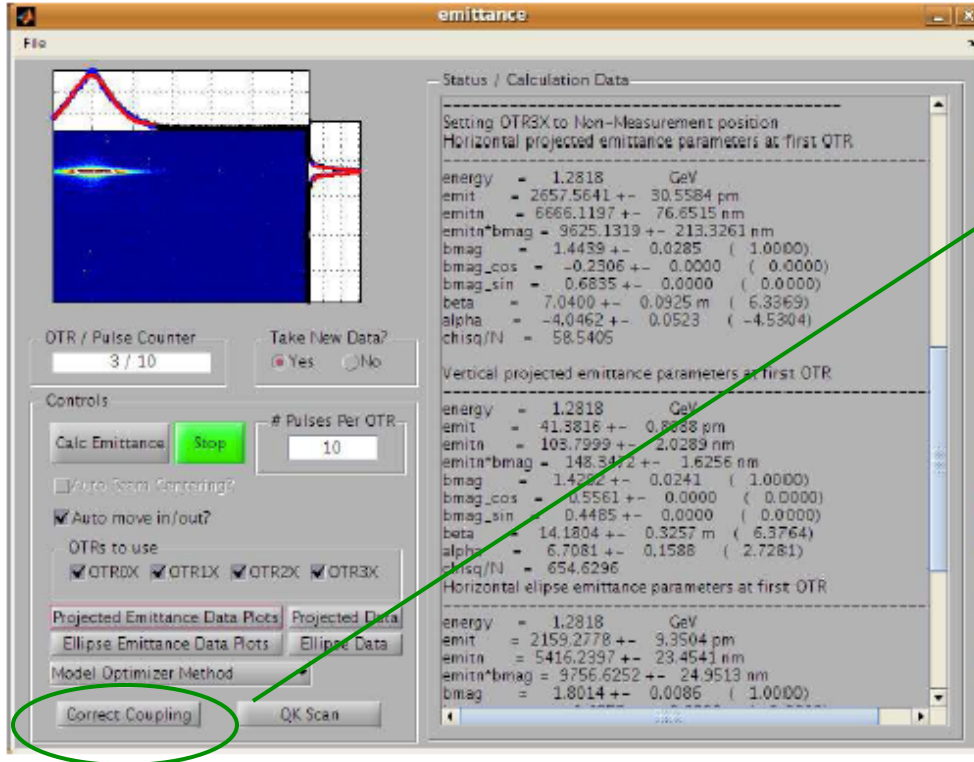


- **Measure the beam size and tilt** in the 4 OTR locations.
- Reconstruct the **beam matrix** upstream at **EXT line entrance** ( $\sigma_0$ ) assuming no coupling and skews switch-off.
- **Transport** it from EXT line entrance to **OTR0** ( $\sigma_i$ ) with the skews switch-on **determining** which **skew strengths** lead to an **uncoupled OTR0** beam matrix (minimise as possible the coupling terms) by solving a 4 equations system with 4 unknowns with constrains in the skew strengths values.

$$R_{0 \rightarrow i} = R_{4 \rightarrow i} R_{skew4} R_{3 \rightarrow 4} R_{skew3} R_{2 \rightarrow 3} R_{skew2} R_{1 \rightarrow 2} R_{skew1} R_{0 \rightarrow 1}$$

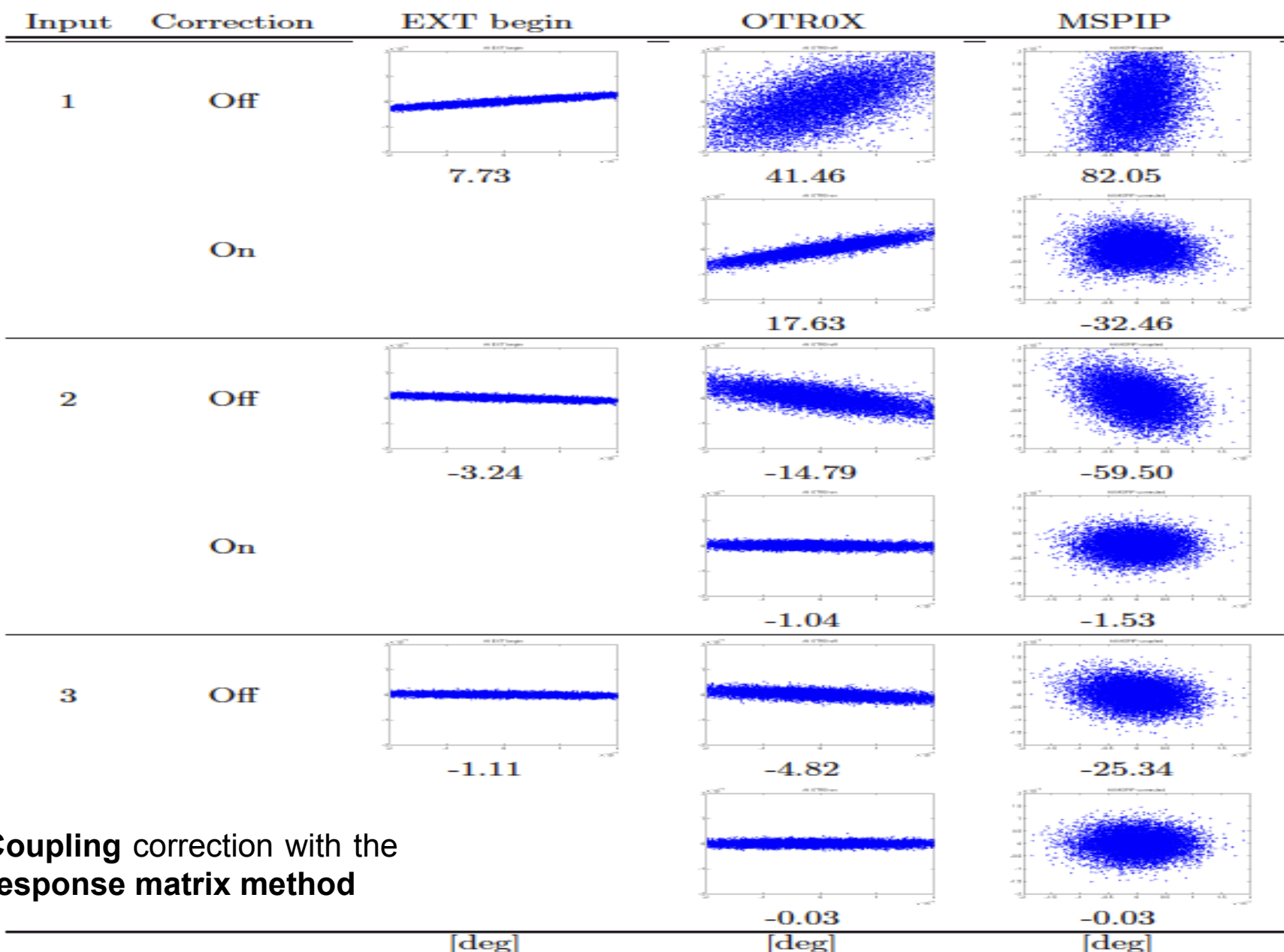


$$R_{0 \rightarrow i} \sigma_0 (R_{0 \rightarrow i})^T = \begin{pmatrix} \sigma_1 & \sigma_2 & \sigma_3 & \sigma_4 \\ \sigma_2 & \sigma_5 & \sigma_6 & \sigma_7 \\ \sigma_3 & \sigma_6 & \sigma_8 & \sigma_9 \\ \sigma_4 & \sigma_7 & \sigma_9 & \sigma_{10} \end{pmatrix}$$



- The **response matrix method coupling** correction method was **installed and tested** in **ATF2 control system** in December 2011
- This gives the possibility to have an **automatic coupling correction** for each nominal lattice using the OTR measurements. The method is **iterative and fast converging**, saving a lot of time in comparison with the standard scanning method.

- Different methods: **scan, response matrix and solve transport matrix** methods have been studied and **compared** with **simulations** and real **measurements**. In comparison with the scan method (non-model dependent), the response method is faster but sometimes present some unstable results.



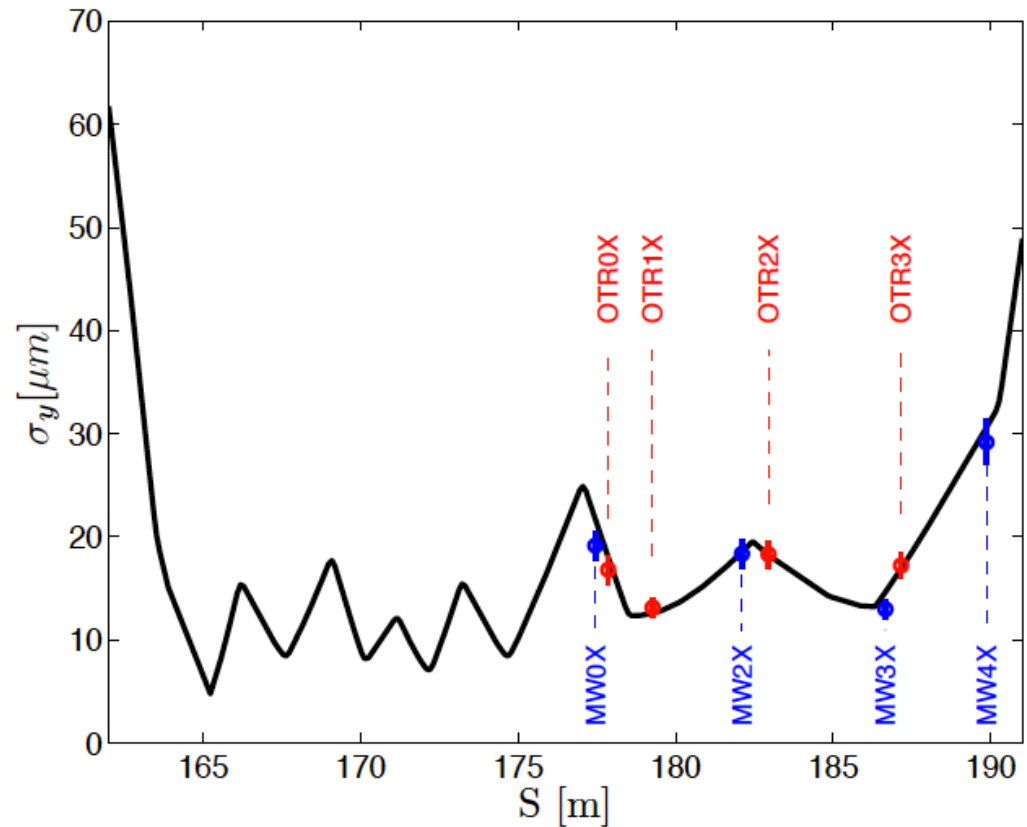
Coupling correction with the response matrix method

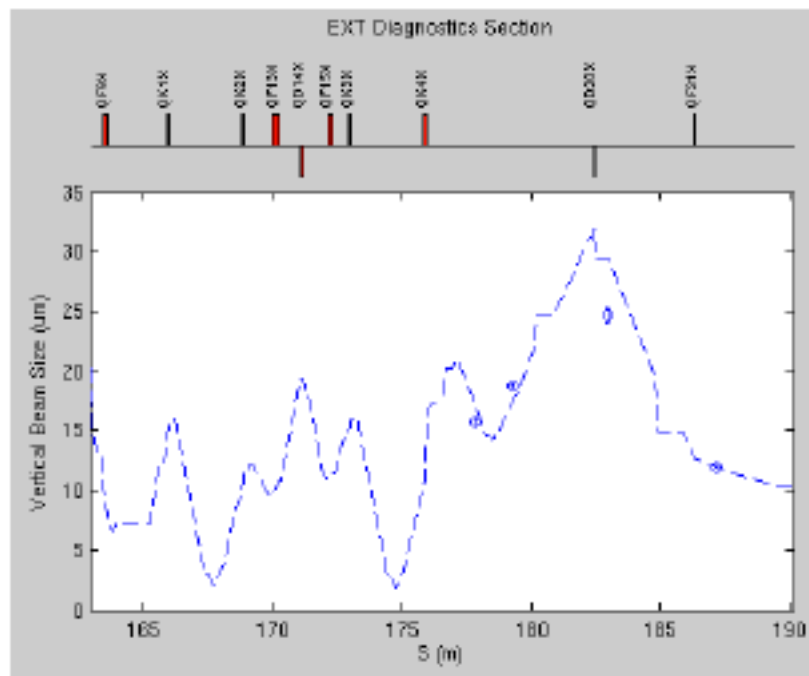
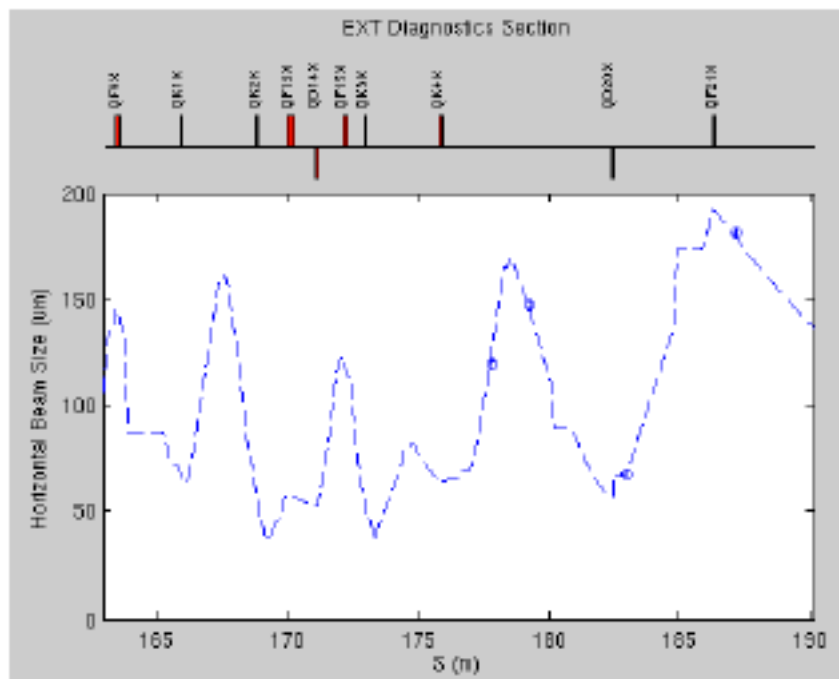
[deg]

[deg]

[deg]

**Comparison** between  
**OTR** and **WS**  
measurements made on  
Dec. 14th 2011

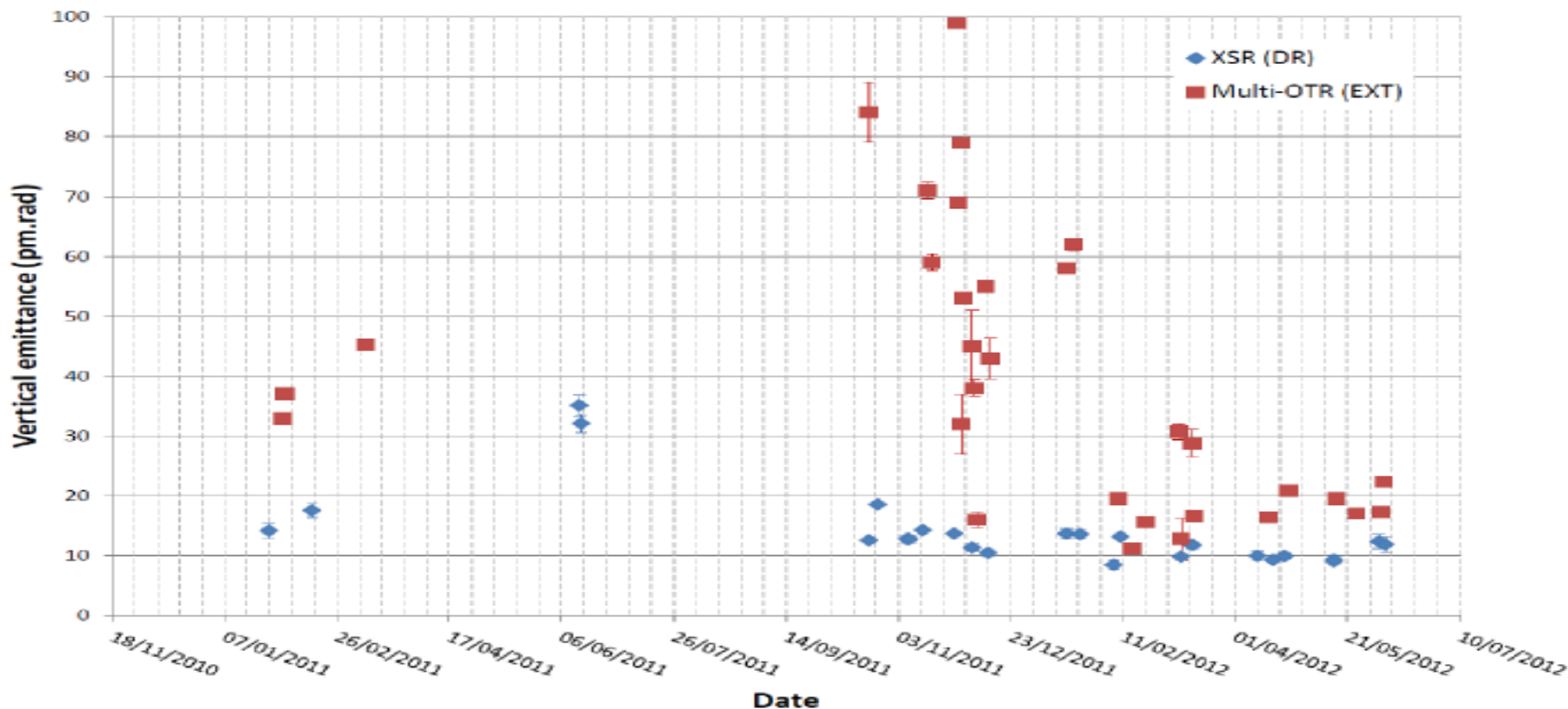




Measurement of the **beam sizes** and **comparison** with the **model** made on 8<sup>th</sup> March 2012

Comparison of **DR** and **EXT** line vertical **emittance** measurements during 2011 and half 2012.

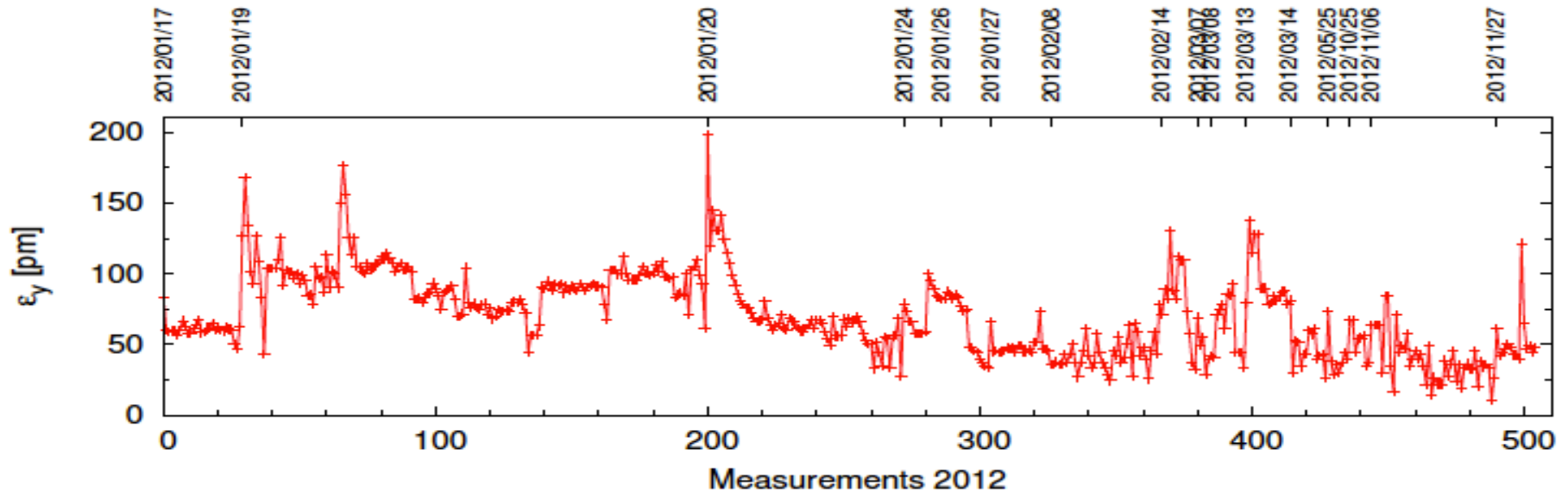
Vertical emittances in DR and EXT line





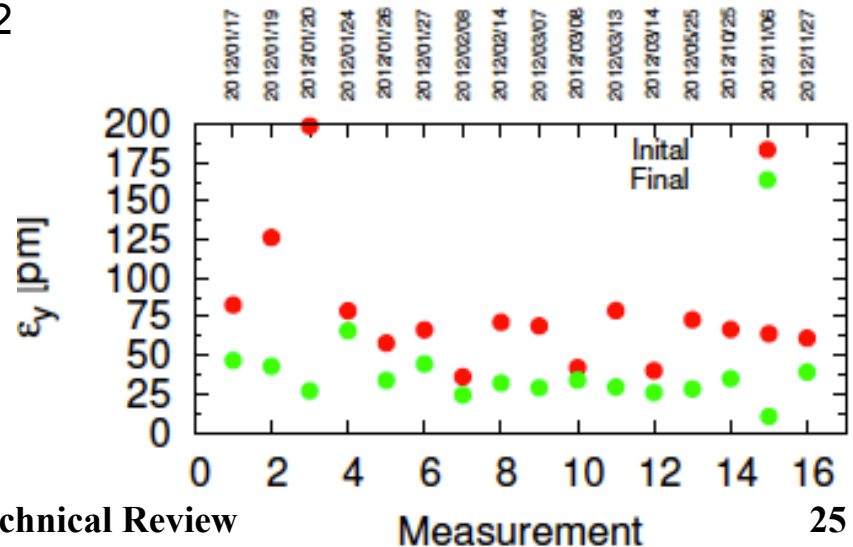
# Beam size and Emittance

## November 2011/December 2012: Systematic Measurements II

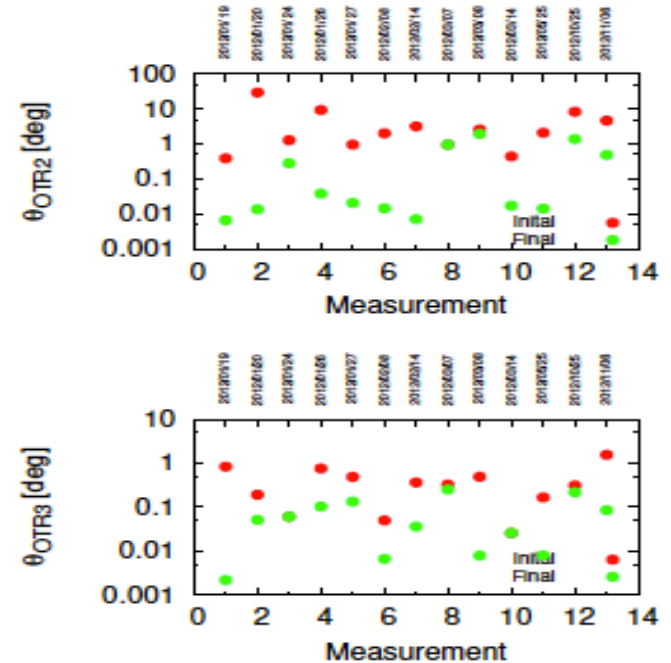
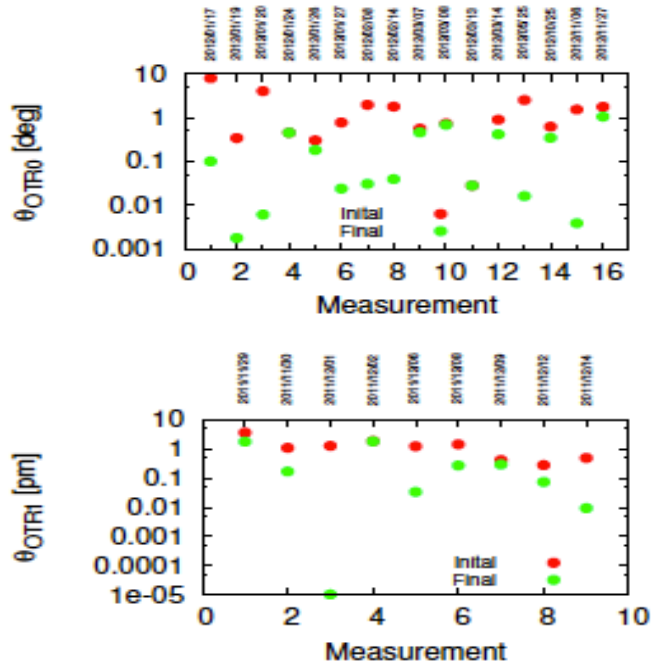


Vertical **emittance** measurements during 2012

- **Initial** (before coupling correction):  
 $\epsilon_y = 76 \pm 39$  pm
- **Final** (after coupling correction):  
 $\epsilon_y = 34 \pm 12$  pm



Beam **Tilts** at OTRs measurements during 2012:



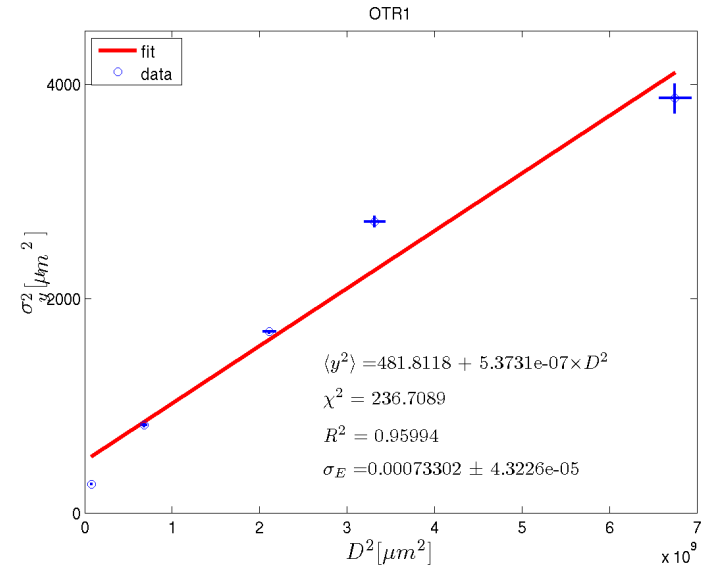
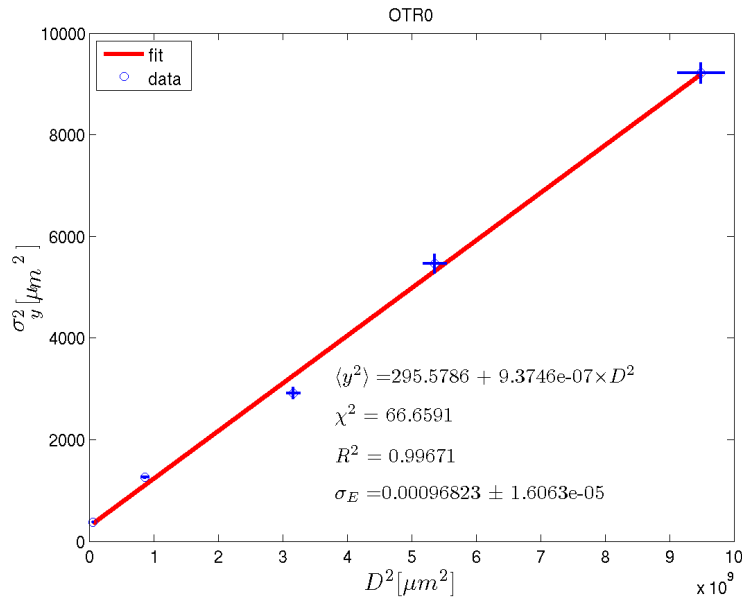
Mean of the |Tilt| values before and after correction:

OTR0  $\Rightarrow \theta_0 = 1.7 \pm 1.9$  deg  
 OTR1  $\Rightarrow \theta_1 = 1.5 \pm 1.7$  deg  
 OTR2  $\Rightarrow \theta_2 = 5.0 \pm 7.6$  deg  
 OTR3  $\Rightarrow \theta_3 = 0.4 \pm 0.4$  deg

Final  $\theta_0 = 0.3 \pm 0.3$  deg  
 Final  $\theta_1 = 0.2 \pm 0.2$  deg  
 Final  $\theta_2 = 0.4 \pm 0.6$  deg  
 Final  $\theta_3 = 0.1 \pm 0.1$  deg

Measured Initial tilts below 10 deg

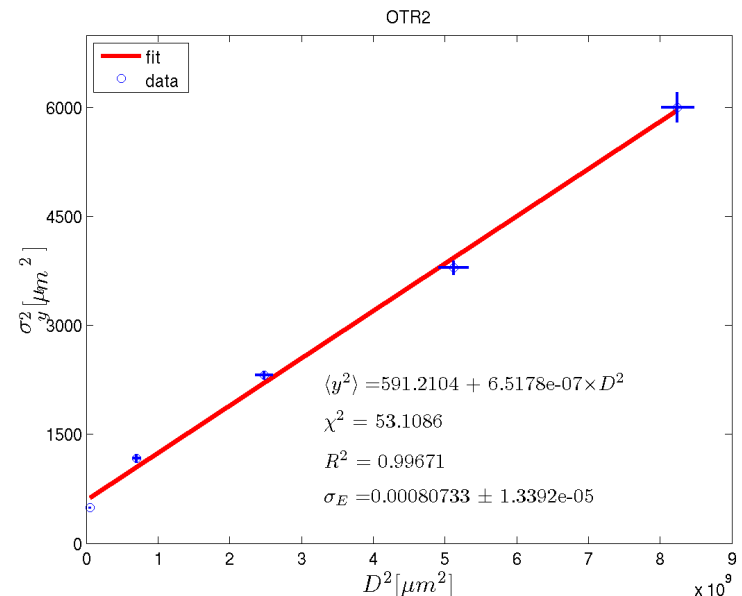
## Energy spread measurement

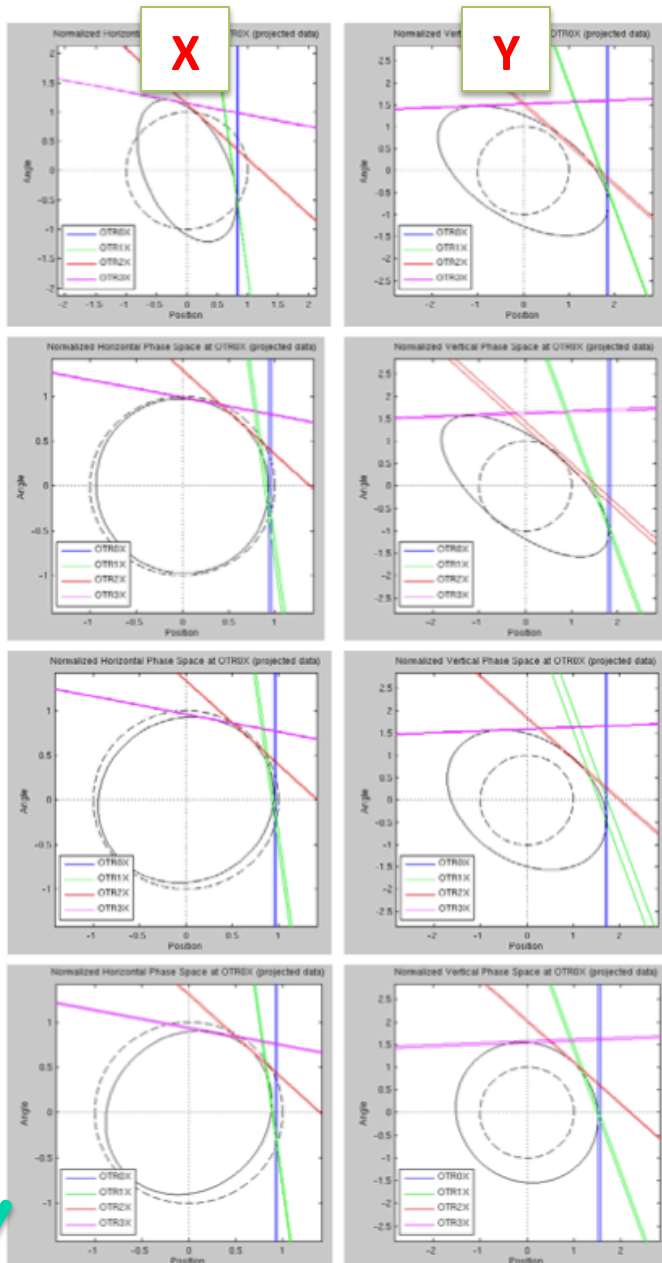


Obtain the **energy spread** by changing the dispersion (QS1X and QS2X) and measuring the change in size

$$\sigma_y^2 = \beta_y \varepsilon_y + D_y^2 \sigma_E^2$$

First measurement:  $\sigma_E = (8.4 \pm 1.2)10^{-4}$





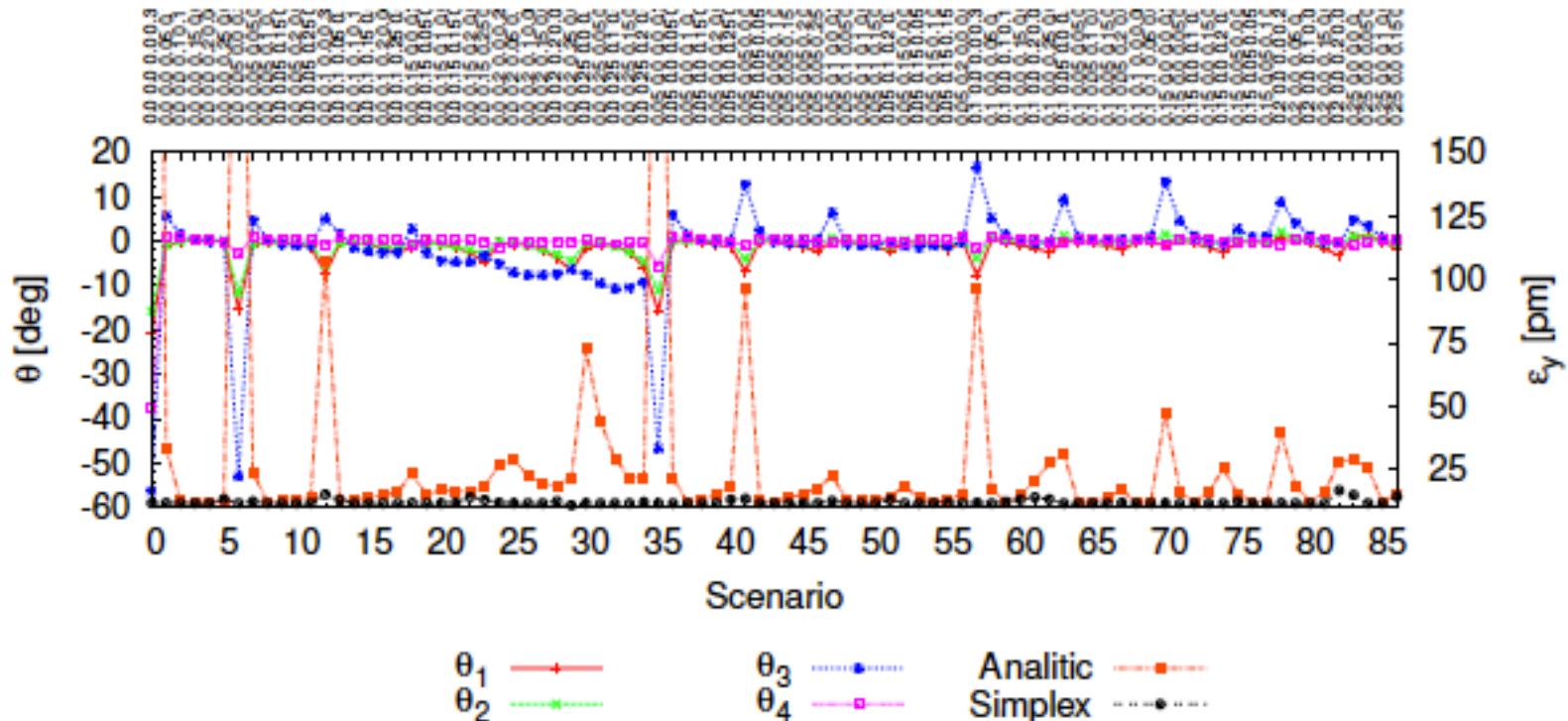
### Beta matching

| name         | match0        | match1        | match2        | match3        | design        |
|--------------|---------------|---------------|---------------|---------------|---------------|
| file         | 054152        | 061717        | 080625        | 084346        |               |
| EmitX        | 1.7894        | 1.8228        | 1.7587        | 1.5860        |               |
| <b>BmagX</b> | <b>1.1946</b> | <b>1.0013</b> | <b>1.0026</b> | <b>1.0076</b> | <b>1.0000</b> |
| EmBmX        | 2.1376        | 1.8251        | 1.7633        | 1.5981        |               |
| BetaX        | 4.7239        | 6.0386        | 6.4327        | 6.2257        | 6.3052        |
| AlphaX       | -2.8890       | -4.2795       | -4.6550       | -4.5596       | -4.4943       |
| EmitY        | 28.4846       | 25.7572       | 30.8175       | 28.2300       |               |
| <b>BmagY</b> | <b>1.2000</b> | <b>1.3489</b> | <b>1.0554</b> | <b>1.0034</b> | <b>1.0000</b> |
| EmBmY        | 34.1808       | 34.7439       | 32.5253       | 28.3262       |               |
| BetaY        | 9.1308        | 9.4923        | 7.1151        | 6.0766        | 6.1903        |
| AlphaY       | 4.4037        | 4.8369        | 3.2854        | 2.6087        | 2.5763        |

- Matching performed using quads in inflector, upstream of OTR system
  - Can easily iterate matching to converge on well matched solution
  - Have to take care not to destroy dispersion & coupling correction system
- Propagate match to IP using online model
- Check match at IP using quad scan technique
  - Scan QD0FF/QF1FF vs. IP Carbon wire scanner
- Typically find good agreement for vertical match at ~10-20% level, a little worse for horizontal

The considered algorithms for correcting the coupling:

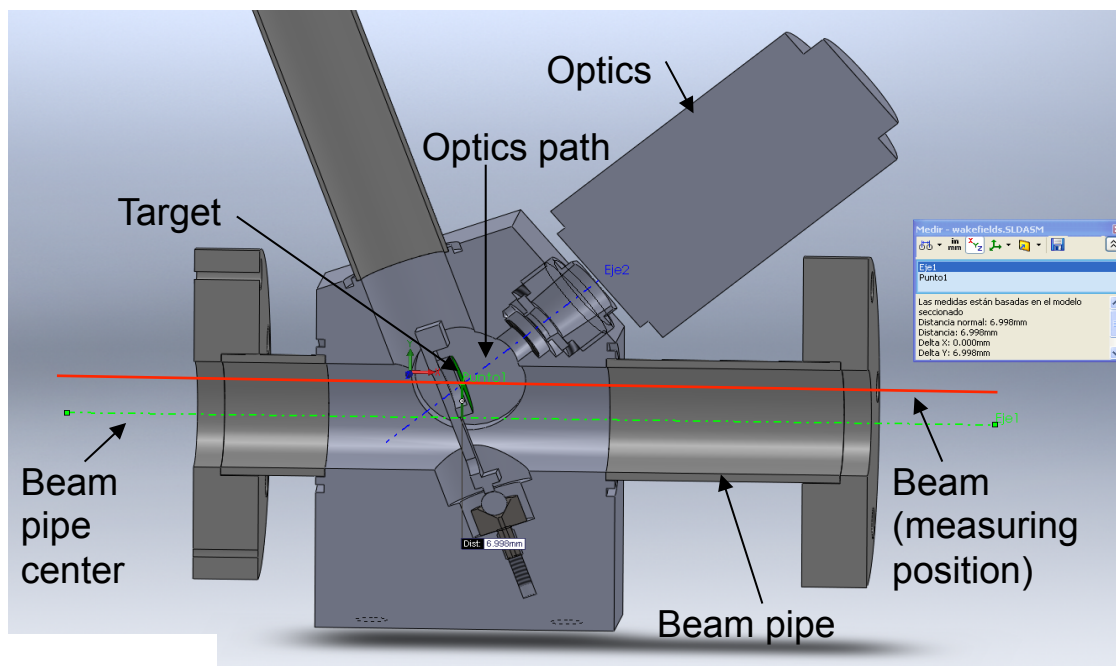
- **Response matrix** method (zeroing the measured tilts of the beam at the OTRs using the strength of 4-skew quadrupoles to compensate the measured tilts at the OTRs)
- **Simplex** algorithm that minimises the **emittance**



**Simplex** is **more efficient** but the cases where the analytical method is not correcting are not realistic in the ATF2 case. With the OTR upgrade the emittance could be measured parasitically and the Simplex method could be **easily implemented**.

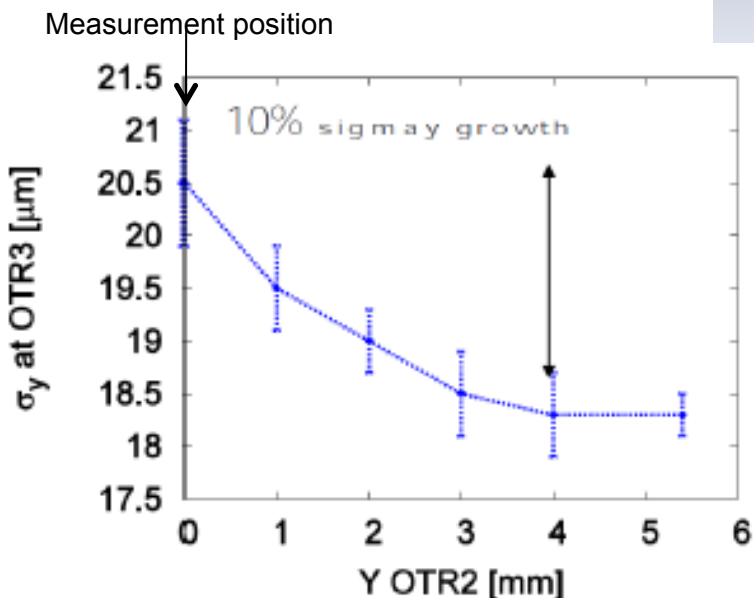
When OTR is not measuring the beam is in the beam pipe centre.

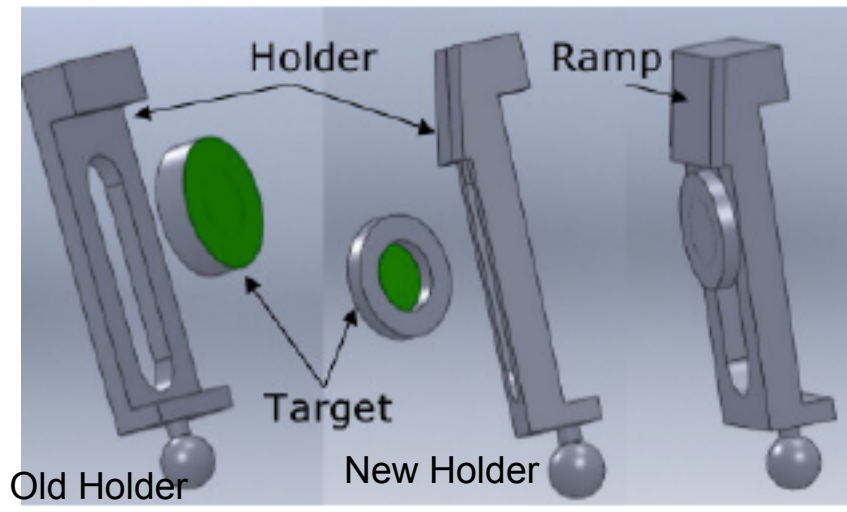
For **measuring** the beam size the mOTR body is **lowered** about **7 mm** for intercepting the beam.



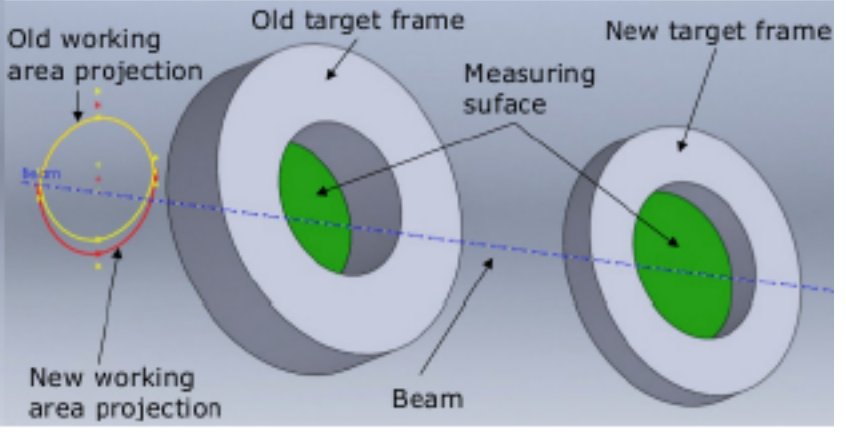
Current target position

**Wakefields** are generated when lowering the OTRs for a **simultaneous measurement**



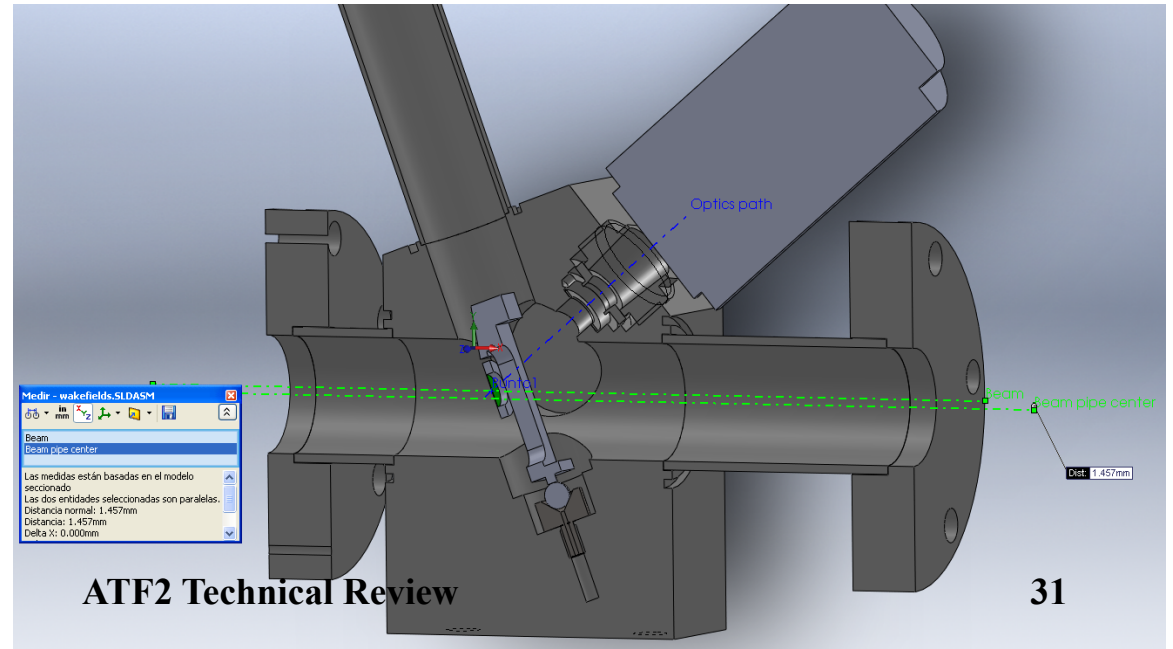


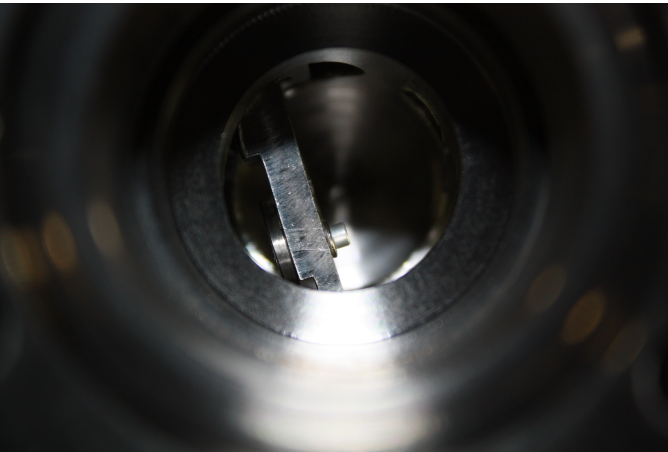
### New Target holder and Target



### New target position

The required distance to be **lowered** for intercepting the beam is reduced from **7 mm** down to **1.5 mm**



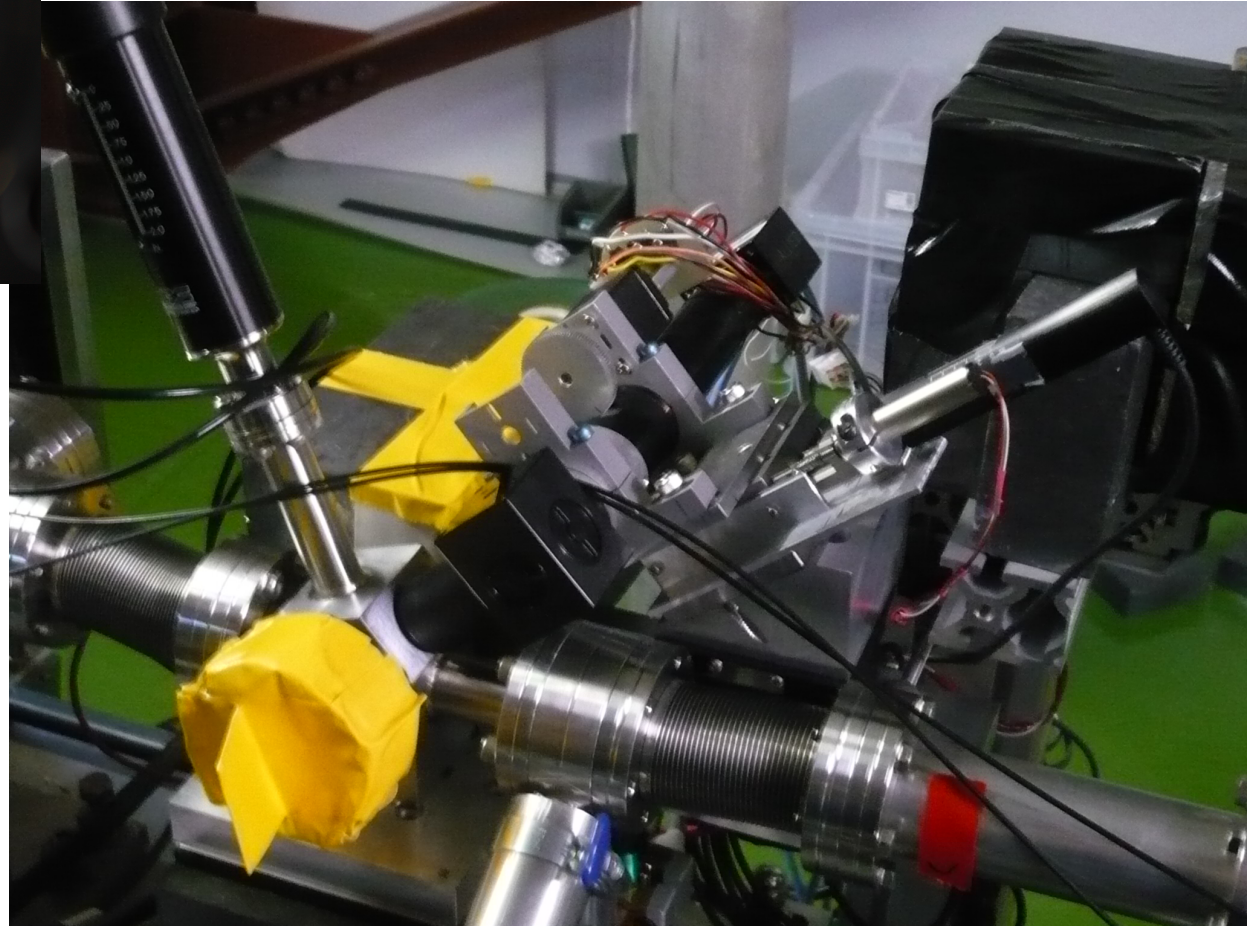


Long working distance target side view

Installation of new target holders and optical system was made in **February 2013**.

Some test has been made after the installation and the system is working properly.

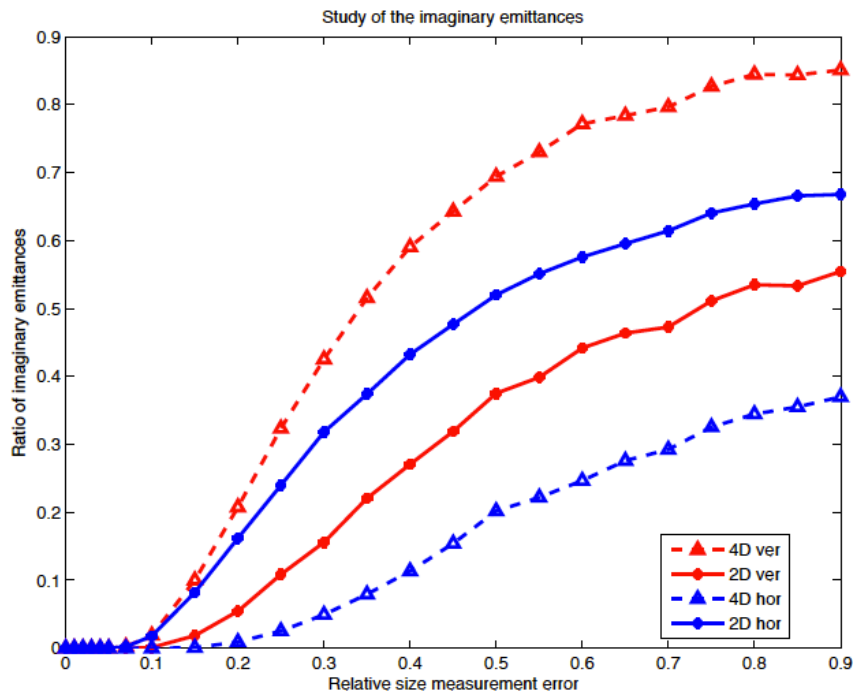
OTR0 long working distance target external view





- The **mOTR** system is the **principal** method to **characterize** the beam in the ATF2 EXT line. Some specific points to be signalled:
  - **Resolution** and **Stability** of the system were well demonstrated by **repeated measurements**
  - **Correctness** of the measurements were demonstrated by **comparison** with previous well tested measurement system the **existing WSs**, also with and additional WS wire embedded into the OTR target devices
  - The **model** fitting and **emittance/twiss calculations** are **corroborated** against the **existing WSs**
  - Achievements and stability of the **emittance**, **coupling** and other **corrections** has been **compared** with **simulations**
- Although the OTR technique is **not new**, the **complete measurement and correction system** of the mOTR system in ATF2 is a **significant evolution** in the state-of-the-art of such solutions. Of special note it is the large degree of **automation** and **integration** with the **online modelling** systems. It represents a highlight of **modern beam instrumentation**. Similar monitor systems can now be deployed at **FLC** and linac-based synchrotron light sources.

The **emittances** could be reconstructed from the **beam size measurements** at different locations along the beamline. The **2D** (transverse) and **4D** (intrinsic) emittances could be obtained by **solving numerically three separated systems** of coupled equations. When the number of measurement stations is greater than four, these **systems are overdetermined**, and the numerical solutions can lead to unphysical results. The incidence of such meaningless results usually increases if the measurements are noisy. Numerical rules can be used to study the conditioning of these systems.



The **main objective** of this work is to **study analytically** the conditions of **solvability of these systems of equations** and its implication in the emittance reconstruction algorithms used in the accelerators. The aim is to give some hints about the **optical constrains** and the **location of the measurement stations**.

# Emittance Reconstruction

## The formalism

The transverse beam envelope matrix:

$$\begin{pmatrix} \sigma_1 & \sigma_2 & \sigma_3 & \sigma_4 \\ \sigma_2 & \sigma_5 & \sigma_6 & \sigma_7 \\ \sigma_3 & \sigma_6 & \sigma_8 & \sigma_9 \\ \sigma_4 & \sigma_7 & \sigma_9 & \sigma_{10} \end{pmatrix} \longrightarrow \begin{pmatrix} \langle x^2 \rangle & \langle xx' \rangle & \langle xy \rangle & \langle xy' \rangle \\ \langle xx' \rangle & \langle xx'^2 \rangle & \langle x'y \rangle & \langle x'y' \rangle \\ \langle xy \rangle & \langle x'y \rangle & \langle y^2 \rangle & \langle yy' \rangle \\ \langle xy' \rangle & \langle x'y' \rangle & \langle yy' \rangle & \langle y'^2 \rangle \end{pmatrix}$$

The projected emittances  
(2D)  $\varepsilon_x$  and  $\varepsilon_y$  are:

$$\begin{array}{c} \text{X submatrix} \\ \begin{pmatrix} \sigma_1 & \sigma_2 & \sigma_3 & \sigma_4 \\ \sigma_2 & \sigma_5 & \sigma_6 & \sigma_7 \\ \sigma_3 & \sigma_6 & \sigma_8 & \sigma_9 \\ \sigma_4 & \sigma_7 & \sigma_9 & \sigma_{10} \end{pmatrix} \\ \text{Y submatrix} \end{array}$$

$$\varepsilon_x = \sqrt{\sigma_1 \sigma_5 - \sigma_2^2}$$

$$\varepsilon_y = \sqrt{\sigma_8 \sigma_{10} - \sigma_9^2}$$

Diagonalization of the beam matrix yields the  
intrinsic emittances  $\varepsilon_1$  and  $\varepsilon_2$  (4D):

$$\begin{pmatrix} \sigma_1 & \sigma_2 & \sigma_3 & \sigma_4 \\ \sigma_2 & \sigma_5 & \sigma_6 & \sigma_7 \\ \sigma_3 & \sigma_6 & \sigma_8 & \sigma_9 \\ \sigma_4 & \sigma_7 & \sigma_9 & \sigma_{10} \end{pmatrix} \longrightarrow \begin{pmatrix} \varepsilon_1 & 0 & 0 & 0 \\ 0 & \varepsilon_1 & 0 & 0 \\ 0 & 0 & \varepsilon_2 & 0 \\ 0 & 0 & 0 & \varepsilon_2 \end{pmatrix}$$

**Experimentally** only the horizontal  $\sigma_1$  vertical  $\sigma_8$  are directly measured. The coupling term  $\sigma_3$  can be deduced by measuring the beam size along a tilted axis at an angle respect to the horizontal beam size.

At least **ten measurements** are required to **reconstruct the beam matrix**. The ten values could be obtained by changing the optics in a controlled manner at the location of the measurements or by **measuring the beam size at different locations**.

Assuming  $N$  measurement stations, for each measurement station labelled as  $i$  one obtain the following **systems of coupled equations**:

$$\begin{aligned}
 \hat{\sigma}_1^{(i)} &= R_{11}^{2(i)} \sigma_1 + 2R_{11}^{(i)} R_{12}^{(i)} \sigma_2 + R_{12}^{2(i)} \sigma_5 \\
 \hat{\sigma}_8^{(i)} &= R_{33}^{2(i)} \sigma_8 + 2R_{33}^{(i)} R_{34}^{(i)} \sigma_9 + R_{34}^{2(i)} \sigma_{10} \\
 \hat{\sigma}_3^{(i)} &= R_{11}^{(i)} R_{33}^{(i)} \sigma_3 + R_{11}^{(i)} R_{34}^{(i)} \sigma_4 + R_{12}^{(i)} R_{33}^{(i)} \sigma_6 + R_{12}^{(i)} R_{34}^{(i)} \sigma_7
 \end{aligned}
 \longrightarrow
 \begin{aligned}
 M_X \begin{pmatrix} \sigma_1 \\ \sigma_2 \\ \sigma_5 \end{pmatrix} &= \begin{pmatrix} \hat{\sigma}_1^{(1)} \\ \hat{\sigma}_1^{(2)} \\ \dots \\ \hat{\sigma}_1^{(N)} \end{pmatrix} &
 M_Y \begin{pmatrix} \sigma_8 \\ \sigma_9 \\ \sigma_{10} \end{pmatrix} &= \begin{pmatrix} \hat{\sigma}_8^{(1)} \\ \hat{\sigma}_8^{(2)} \\ \dots \\ \hat{\sigma}_8^{(N)} \end{pmatrix} &
 M_{XY} \begin{pmatrix} \sigma_3 \\ \sigma_4 \\ \sigma_6 \\ \sigma_7 \end{pmatrix} &= \begin{pmatrix} \hat{\sigma}_3^{(1)} \\ \hat{\sigma}_3^{(2)} \\ \dots \\ \hat{\sigma}_3^{(N)} \end{pmatrix}
 \end{aligned}$$

- with **3** stations only the projected emittance (**2D**) could we reconstructed
- with **4** stations **coupled** beam matrix could be reconstructed but the first two systems are **overdetermined**
- with **>4** stations **coupled** beam matrix could be reconstructed but the three systems are **overdetermined**.

# Emittance Reconstruction Analytical conditions: Projected Emittance (2D)

In the general case of  $N$  measurement stations. The system has **unique solution** ( $\sigma_1 \sigma_2 \sigma_3$ ) if and only if the rank of both  $M_x$  and  $M_x^*$  is equal to three. This give us two conditions:

**Condition1:**  $\phi_x^{(ji)} \neq n\pi, \forall(i, j)$

The **measurement** stations should be **located** at places where the **phase advances** correspond to **different snapshots** of the beam. This is the only required condition in the case of **3** measurement stations.

For **4 or more stations** a second condition is required to get a unique solution.

**Condition 2:**  $-\hat{\sigma}_1^{(i)} \Delta_{3x}(jkl) + \hat{\sigma}_1^{(j)} \Delta_{3x}(ikl) - \hat{\sigma}_1^{(k)} \Delta_{3x}(ijl) + \hat{\sigma}_1^{(l)} \Delta_{3x}(ijk) = 0, \forall(ijkl)$

$$\Delta_{3x}(ijk) = 2\beta_x^{(i)} \beta_x^{(j)} \beta_x^{(k)} \sin\phi_x^{(ji)} \sin\phi_x^{(ki)} \sin\phi_x^{(kj)}$$

$$A_{4x}(ijkl) = -\hat{\sigma}_1^{(i)} \Delta_{3x}(jkl) + \hat{\sigma}_1^{(j)} \Delta_{3x}(ikl) - \hat{\sigma}_1^{(k)} \Delta_{3x}(ijl) + \hat{\sigma}_1^{(l)} \Delta_{3x}(ijk)$$

Condition 2 involve the  $\beta$  and the **measurements**, one can see that **in general** the **equality cannot be exactly satisfied**. One could replace the **zero** by some previously **fixed error value**, related with the error of the **measurements**.

**Idem for vertical plane.**

In the general case of  $N$  measurement stations we have  $M_{XY}$  and  $M_{XY}^*$ , the system has **unique solution**  $(\sigma_3 \sigma_4 \sigma_6 \sigma_7)$  if and only if the rank of both  $M_{XY}$  and  $M_{XY}^*$  is equal to four. This give us two more conditions:

**Condition 3:**

$$\begin{aligned} & \cos(\varphi_x^{(ji)} + \varphi_x^{(lk)}) [\cos(\varphi_y^{(ki)} + \varphi_y^{(lj)}) - \cos(\varphi_y^{(ki)} - \varphi_y^{(lj)})] \\ & + \cos(\varphi_x^{(ki)} + \varphi_x^{(lj)}) [\cos(\varphi_y^{(ji)} - \varphi_y^{(lk)}) - \cos(\varphi_y^{(ji)} + \varphi_y^{(lk)})] \\ & + \cos(\varphi_x^{(ji)} - \varphi_x^{(lk)}) [\cos(\varphi_y^{(ji)} + \varphi_y^{(lk)}) - \cos(\varphi_y^{(ki)} + \varphi_y^{(lj)})] \neq 0, \forall (ijkl) \end{aligned}$$

This is the only required condition in the case of **4** measurement stations. In the particular case where  $\phi_x^{(ji)} = \phi_y^{(ji)}$  the system has **no solution**.

For **5 or more stations** an additional condition is required to get a **unique solution**.

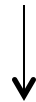
**Condition 4:**  $\hat{\sigma}_3^{(i)} \Delta_4(jklm) - \hat{\sigma}_3^{(j)} \Delta_4(iklm) + \hat{\sigma}_3^{(k)} \Delta_4(ijlm) - \hat{\sigma}_3^{(l)} \Delta_4(ijkm) + \hat{\sigma}_3^{(m)} \Delta_4(ijkl) = 0, \forall (ijklm)$

$$\begin{aligned} & -8(\beta_x^{(i)} \beta_y^{(i)} \beta_x^{(j)} \beta_y^{(j)} \beta_x^{(k)} \beta_y^{(k)} \beta_x^{(l)} \beta_y^{(l)})^{-1/2} \Delta_4(ijkl) = \cos(\varphi_x^{(ji)} + \varphi_x^{(lk)}) [\cos(\varphi_y^{(ki)} + \varphi_y^{(lj)}) - \cos(\varphi_y^{(ki)} - \varphi_y^{(lj)})] \\ & + \cos(\varphi_x^{(ki)} + \varphi_x^{(lj)}) [\cos(\varphi_y^{(ji)} - \varphi_y^{(lk)}) - \cos(\varphi_y^{(ji)} + \varphi_y^{(lk)})] + \cos(\varphi_x^{(ji)} - \varphi_x^{(lk)}) [\cos(\varphi_y^{(ji)} + \varphi_y^{(lk)}) - \cos(\varphi_y^{(ki)} + \varphi_y^{(lj)})] \end{aligned}$$

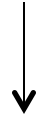
One could replace the **zero** by some previously **fixed error value**, related with the error of the **measurements**.

- We have studied **analytically** the conditions of **solvability of the systems** of equations involved in the process of emittance reconstruction and we have obtained some **conditions** about the **locations** of the measurements to avoid unphysical results.
- These conditions have been **tested analytically** in various systems as in the NLC diagnostic section and in **ATF2 EXT line**, giving good results. **Simulations** are being made to test the robustness in **high coupling scenarios** and **large measurement errors**.
- The results of these studies will be very **useful** to better **determine** the **location** of the **emittance measurement stations** in the diagnostic sections of FLCs.

The **m-OTR system** of the ATF2 EXT line has **demonstrated** its performances as a fast (1min) and **reliable system** to measure the beam size and the emittance. The system is **totally integrated** in the **online model** and it is **crucial** for **tuning procedures** of the beamline as: coupling correction, beta matching, energy spread measurements...



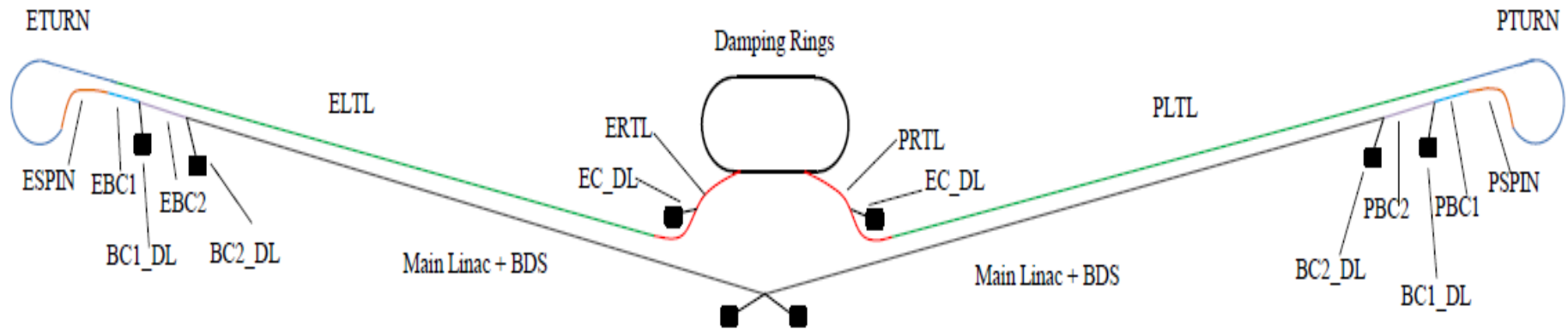
- OTR monitors are **mature** and **reliable diagnostic** tools that could be very suitable for the setup and tuning of the machine in single-bunch mode. It can be very useful during start up and commissioning phases of the **ILC RTML**



- We explore the **feasibility** of using a **m-OTR system** in **transfer lines** of the **ILC RTML**
- We investigate different **materials** for the **OTR target** and possible limitations of operation

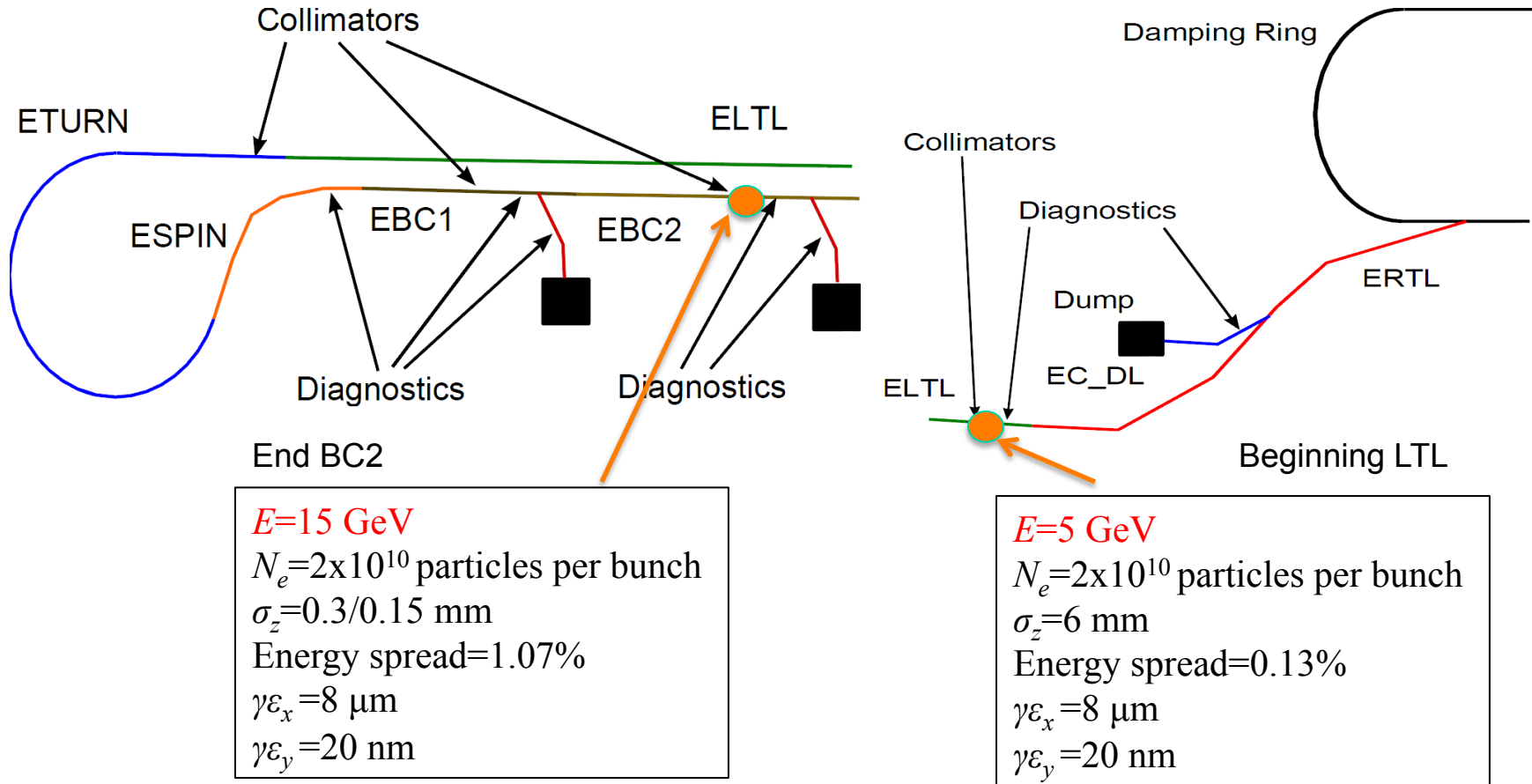


## ILC RTML beamlines



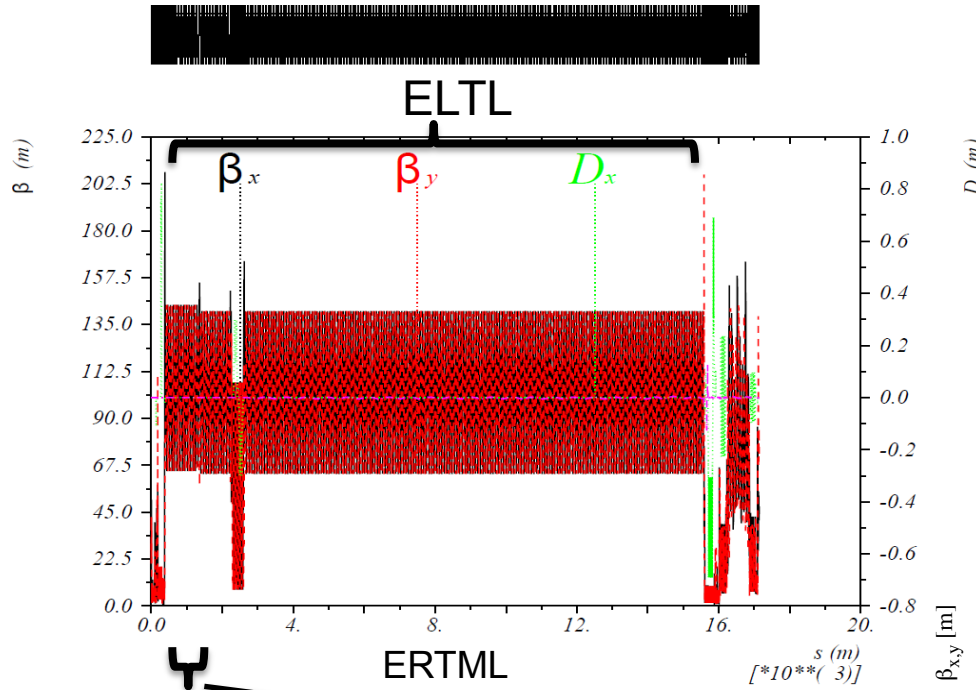
- **ERTL/PRTL**:  $e^-/e^+$  Ring-to-Line from DR to Main Tunnel (+ Dump Line)
- **ELTL/PLTL**:  $e^-/e^+$  Long-Transfer-Line
- **ETURN/PTURN**:  $e^-/e^+$  Turn-Around
- **ESPIN/PSPIN**:  $e^-/e^+$  Spin rotator
- **EBC1/PBC1**:  $e^-/e^+$  1<sup>st</sup> stage of Bunch Compressor (+ Dump Line)
- **EBC2/PBC2**:  $e^-/e^+$  2<sup>nd</sup> stage of Bunch Compressor (+ Dump Line)

### Possible positions for m-OTR systems

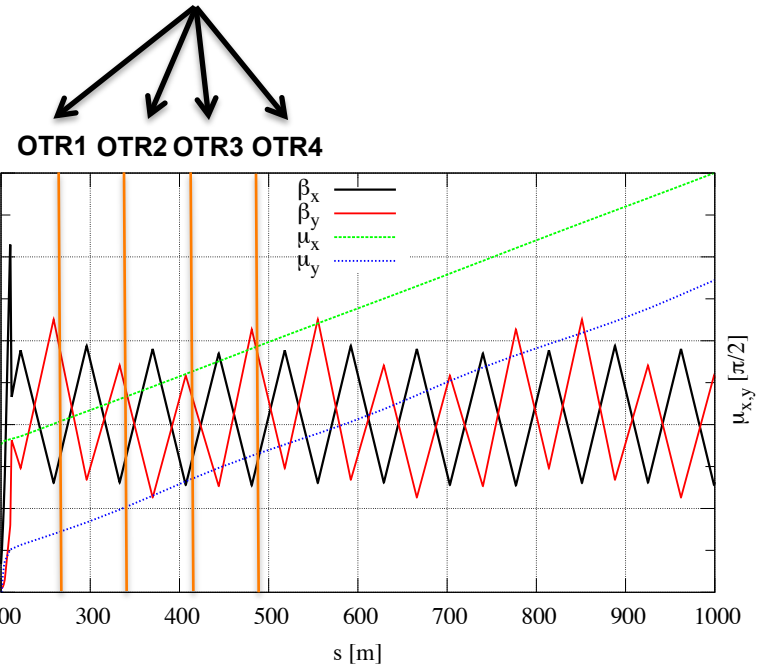


ILC RTML has been designed with 7 diagnostic sections: beginning of LTL, end of spin rotator SPIN, end of BC1 and BC2 and in each extraction line

### RTML Long Transfer Line



Beginning LTL: 4 OTRs monitors



$E=5 \text{ GeV}$   
 $N_e=2 \times 10^{10}$  particles per bunch  
 $\sigma_z=6 \text{ mm}$   
 Energy spread=0.13%  
 $\gamma \epsilon_x=8 \text{ } \mu\text{m}$   
 $\gamma \epsilon_y=20 \text{ nm}$

### OTR target study for beginning LTL : Temperature rise of material per pulse

- Peak of instantaneous temperature rise:

$$\Delta T_{inst} = \frac{1}{\rho C_p} \left( \frac{dE}{dz} \right) \frac{N_b N_e}{2\pi \sigma_x \sigma_y}$$

- $\rho$ : material density
- $C_p$ : specific heat
- $N_b$ : number of bunches per pulse ( $N_b=1$ , single bunch mode)
- $N_e$ : number of particles per bunch ( $N_e=2 \times 10^{10}$ )
- $\sigma_x \approx 239.14 \mu\text{m}$ ,  $\sigma_y \approx 17.49 \mu\text{m}$  ( $\beta_x \approx 70 \text{ m}$ ,  $\beta_y \approx 150 \text{ m}$ )
- $dE/dz$ : Collision stopping power in a thin material ( $< X_0$ ) (calculated from the Bethe-Bloch formula)

- Comparison with fracture limit due to thermal stress:

- $\sigma_{UTS}$ : ultimate tensile stress
- $\alpha_T$ : thermal expansion coefficient
- $Y$ : Young modulus

$$\Delta T_{fr} \cong \frac{2\sigma_{UTS}}{\alpha_T Y}$$

| Material | $\frac{1}{\rho} \frac{dE}{dz}$ | $\frac{\text{MeV} \cdot \text{cm}^2}{g}$ | Density $\rho$ g/cm <sup>3</sup> | $\frac{dE}{dz}$ [ $\frac{\text{MeV}}{\text{cm}}$ ] | $\Delta T_{inst}$ [K] | $\Delta T_{fr}$ [K] | $T_{melt}$ [K]                     |
|----------|--------------------------------|--|----------------------------------|--|-----------------------|---------------------|------------------------------------|
| Kapton   | 2.322                          |  | 1.42                             | 2.297  | 18.096                | 9240                | Does not melt, decomposes at 793 K |
| Al       | 2.14                           |  | 2.7                              | 5.778  | 28.675                | 63.662              | 933.37                             |
| Be       | 2.002                          |  | 1.85                             | 3.704  | 12.682                | 222.28              | 1546                               |
| Ti       | 2.007                          |  | 4.54                             | 9.112  | 46.35                 | 441.06              | 1923                               |
| W        | 1.677                          |  | 19.3                             | 32.366   | 152.6                 | 1059.7              | 3643                               |

For all the cases studied:  $\Delta T_{inst} < \Delta T_{fr}$  (fracture limit) and  $T_{melt}$  (melting point),

**No damage operating in low charge (single bunch) mode**

### OTR target study for beginning LTL: Long Term heating

Heat transfer by conduction in a cylindrical system (OTR target) for a Gaussian bunch and thin targets

- The equilibrium temperature:

$$\Delta T_{eq} = T(0) - T(R) = \frac{dE}{dz} \cdot \frac{N_b N_e f_{rep}}{4\pi k} \ln \left( \frac{R^2}{2\sigma_r^2} \right)$$

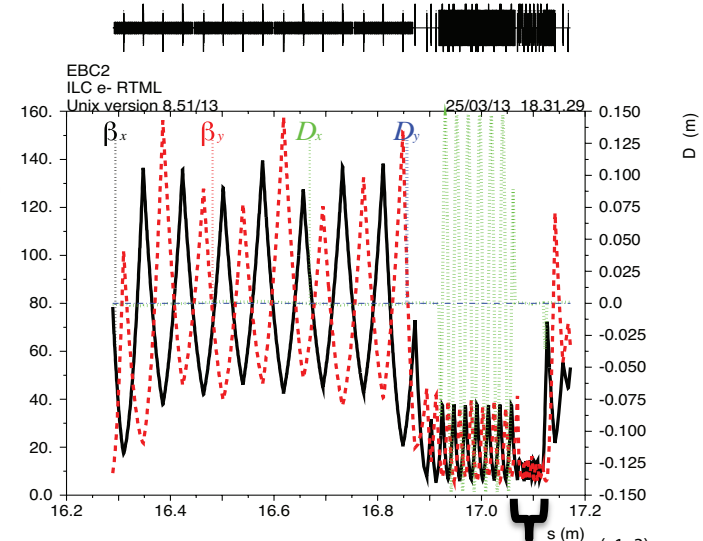
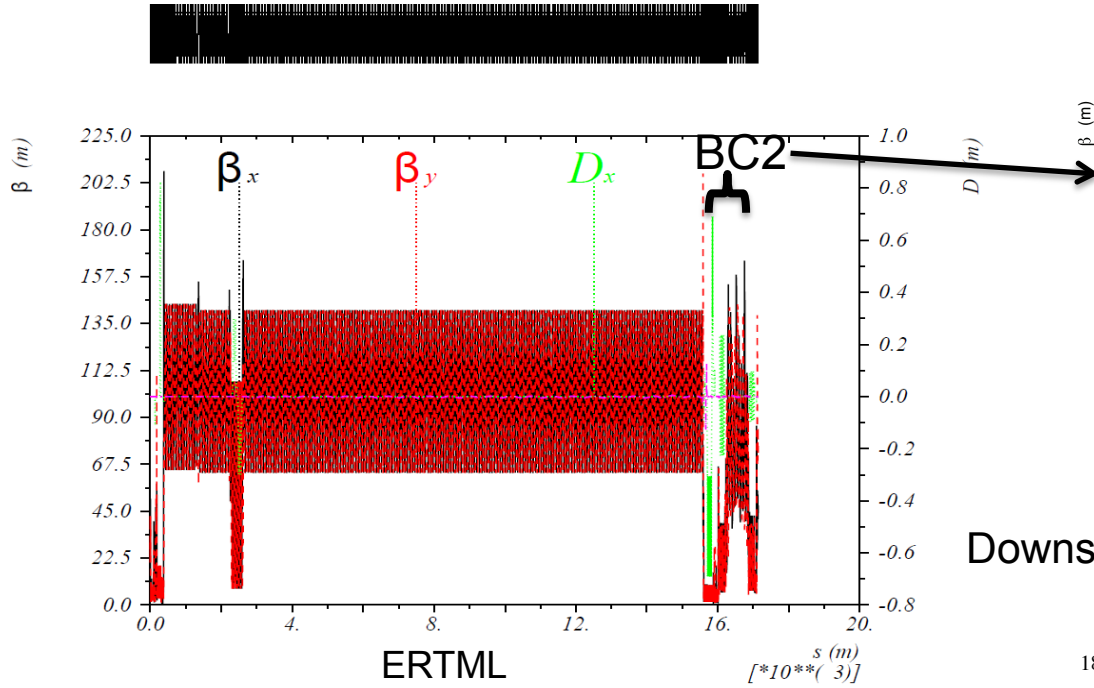
Target radius  $R=6$  mm (same as for ATF2 OTR prototype)  
 Repetition frequency  $f_{rep}=5$  Hz  
 $k$ : thermal conductivity  
 $\sigma_r^2 = \sqrt{(\sigma_x \sigma_y)}$

| Material | $k$ [ $\text{W} \cdot \text{m}^{-1} \cdot \text{K}^{-1}$ ] | $\frac{dE}{dz}$ [ $\frac{\text{MeV}}{\text{cm}}$ ] | $\Delta T_{eq}$ [K] |
|----------|--|--|---------------------|
| Kapton   | 0.12   | 2.297  | 20.42               |
| Al       | 210  | 5.778  | 0.03                |
| Be       | 200  | 3.704  | 0.02                |
| Ti       | 17   | 9.112  | 0.57                |
| W        | 163  | 32.366   | 0.21                |

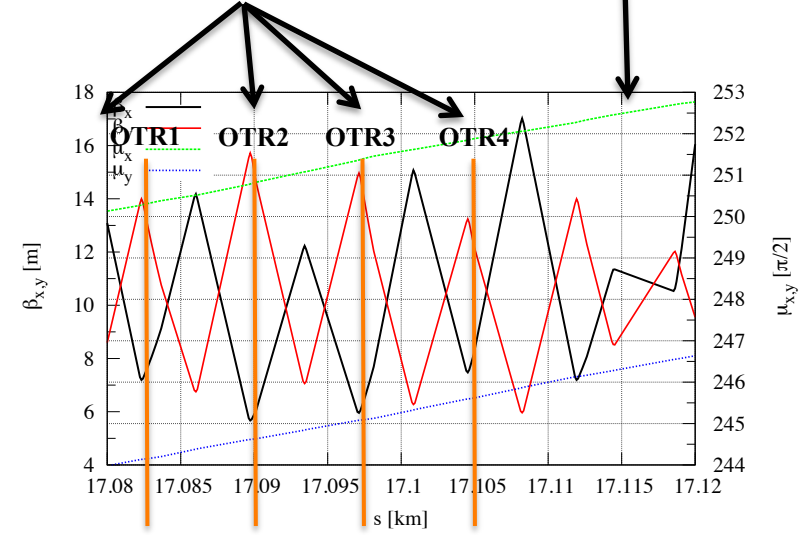
Over many pulses (1 bunch each) these materials have no problem because they conduct the heat appearing in the beam area very quickly to the rest of the target.

**No damage**

## RTML BC2



Downstream of BC2, in the linac launch 4OTRs



$E=15$  GeV  
 $N_e=2 \times 10^{10}$  particles per bunch  
 $\sigma_z=0.3/0.15$  mm  
 Energy spread=1.07%  
 $\gamma\epsilon_x=8$   $\mu\text{m}$   
 $\gamma\epsilon_y=20$  nm

## OTR target study for end BC2 : Temperature rise of material per pulse

- Peak of instantaneous temperature rise:
 
$$\Delta T_{inst} = \frac{1}{\rho C_p} \left( \frac{dE}{dz} \right) \frac{N_b N_e}{2\pi \sigma_x \sigma_y}$$
  - $\rho$ : material density
  - $C_p$ : specific heat
  - $N_b$ : number of bunches per pulse ( $N_b=1$ , single bunch mode)
  - $N_e$ : number of particles per bunch ( $N_e=2 \times 10^{10}$ )
  - $\Sigma_x \approx 75.62 \mu\text{m}$ ,  $\sigma_y \approx 5.34 \mu\text{m}$  ( $\beta_x \approx 7 \text{ m}$ ,  $\beta_y \approx 14 \text{ m}$ )
  - $dE/dz$ : Collision stopping power in a thin material ( $< X_0$ ) (calculated from the Bethe-Bloch formula)
- Comparison with fracture limit due to thermal stress:
 
$$\Delta T_{fr} \cong \frac{2\sigma_{UTS}}{\alpha_T Y}$$
  - $\sigma_{UTS}$ : ultimate tensile stress
  - $\alpha_T$ : thermal expansion coefficient
  - $Y$ : Young modulus

| Material | $\frac{1}{\rho} \frac{dE}{dz}$ | $\frac{\text{MeV}\cdot\text{cm}^2}{\text{g}}$ | Density $\rho$ g/cm <sup>3</sup> | $\frac{dE}{dz}$ [ $\frac{\text{MeV}}{\text{cm}}$ ] | $\Delta T_{inst}$ [K] | $\Delta T_{fr}$ [K] | $T_{melt}$ [K]                     |
|----------|--------------------------------|---|----------------------------------|--|-----------------------|---------------------|------------------------------------|
| Kapton   | 2.58                           |   | 1.42                             | 3.665  | 298.81                | 9240                | Does not melt, decomposes at 793 K |
| Al       | 2.22                           |   | 2.7                              | 5.996  | 307.96                | 63.662              | 933.37                             |
| Be       | 2.066                          |   | 1.85                             | 3.822  | 135.43                | 222.28              | 1546                               |
| Ti       | 2.067                          |   | 4.54                             | 9.386  | 494.12                | 441.06              | 1923                               |
| W        | 1.745                          |   | 19.3                             | 33.678   | 1643.3                | 1059.7              | 3643                               |

In this case, stress fractures may be generated for targets made of Al, Ti and W. In principle, these calculations indicate that Kapton and Be might avoid damage. However, the use of Be could be discouraged due to costs and difficulties of machining (toxicity). **Kapton could be a good candidate!**

## OTR target study for end BC2 : Long Term heating

Heat transfer by conduction in a cylindrical system (OTR target) for a Gaussian bunch and thin targets

- The equilibrium temperature:

$$\Delta T_{eq} = T(0) - T(R) = \frac{dE}{dz} \cdot \frac{N_b N_e f_{rep}}{4\pi k} \ln \left( \frac{R^2}{2\sigma_r^2} \right)$$

Target radius  $R=6$  mm (same as for ATF2 OTR prototype)  
 Repetition frequency  $f_{rep}=5$  Hz  
 $k$ : thermal conductivity  
 $\sigma_r^2 = \sqrt{(\sigma_x \sigma_y)}$

| Material | $k$ [W·m <sup>-1</sup> ·K <sup>-1</sup> ] | $\frac{dE}{dz}$ [ $\frac{\text{MeV}}{\text{cm}}$ ] | $\Delta T_{eq}$ [K] |
|----------|---|--|---------------------|
| Kapton   | 0.12                                      | 3.665  | 41.68               |
| Al       | 210                                       | 5.996  | 0.04                |
| Be       | 200                                       | 3.822  | 0.03                |
| Ti       | 17  | 9.386  | 0.75                |
| W        | 163                                       | 33.678   | 0.28                |

Over many pulses (1 bunch each) these materials have **no problem** because they conduct the heat appearing in the beam area very quickly to the rest of the target. Therefore the long term heating (assuming 5 Hz pulse repetition frequency) is not a problem. The real problem is caused by the thermal stress during the instantaneous deposition of energy.



# Final Conclusions

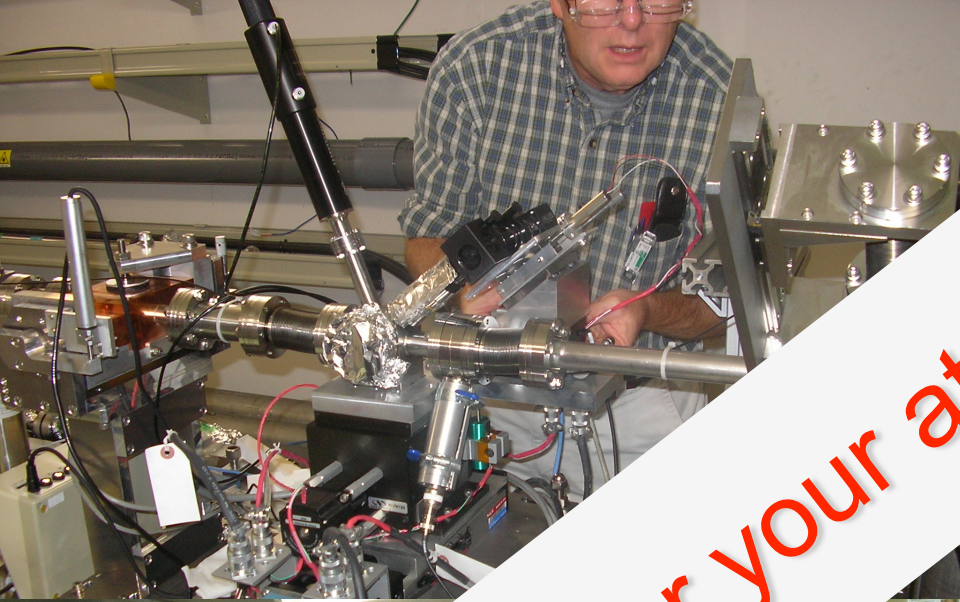
---

- The **m-OTR system** of the ATF2 EXT has demonstrated its performances as a **fast** (1min) and **reliable** system for measuring the beam size and the emittance. The system is **totally integrated** in the **online model** and it is **crucial** for **tuning procedures** of the beamline as: coupling correction, beta matching, energy spread measurements...Studies to ameliorate these procedures are under study
- A **systematic measurement campaign** to determine if the new target configuration is able to avoid the **wakefield effect** of the **simultaneous measurement** of the 4 OTRs has to be made and also a **intensity beam size dependence** measurement and its implications in the resolution
- We have **studied analytically** the **conditions of solvability** of the systems of equations involved in the process of emittance reconstruction and we have obtained some rules about the **locations** of the **measurement stations** to avoid unphysical results. **Simulations** are being made to test the robustness with high coupling scenarios and measurement errors. The results of these studies will be very **useful** to better determine the location of the emittance measurement stations in the **diagnostic sections** of **FLCs**.
- OTR monitors are **mature** and **reliable** diagnostic tools that could be **very suitable** for the setup and tuning of the machine in single-bunch mode. It can be very useful during **start up** and **commissioning** phases of the **RTML**. The **feasibility** of using a m-OTR system in **transfer lines** of the **ILC RTML** as well as a study of the different **materials** for the OTR **target** and possible limitations of operation is ongoing.

# References

---

- [1] ATF Collaboration, *Present status of the final focus beam line at the KEK Accelerator Test Facility*. Physical Review Special Topics Accelerators and Beams 13, 042801 (2010).
- [2] ATF collaboration, *Instrumentation for the ATF2 Facility*. IPAC10.
- [3] J. Alabau Gozalvo, C. Blanch, A. Faus-Golfe, J.V. Civera, J.J. Garcia-Garrigos, D. McCormick, G. White, J. Cruz, *Multi Optical Transition Radiation System for ATF2*. IPAC10.
- [4] J. Alabau Gonzalvo, C. Blanch-Gutiérrez, A. Faus-Golfe, J. J. García-Garrigos, D. McCormick, J. Cruz, M. Woodley, G. White, *Multi Optical transition Radiation System for ATF2*, DIPAC2011
- [5] J. Alabau-Gonzalvo, C. Blanch Gutierrez, A. Faus-Golfe, J. J. Garcia-Garrigos , J. Cruz, D. McCormick, G. White, M. Woodley, *Optical Transition Radiation System for ATF2*, IPAC2011.
- [6] J. Alabau Gozalvo, C. Blanch, A. Faus-Golfe, D. McCormick, G. White, J. Cruz M. Woodley, *Multi-OTR system for ATF2*, Physics Procedia TIPP2011.
- [7] J. Alabau-Gonzalvo, C. Blanch-Gutierrez, J. Cruz, A. Faus-Golfe, J. J. Garcia-Garrigos, D. McCormick, J. Resta-Lopez, G. White, M. Woodley, *Optics and Emittance Studies Using the ATF2 Multi-OTR System*. IPAC2012, New Orleans, Louisiana, USA, 2012.
- [8] J. Alabau-Gonzalvo, C. Blanch-Gutierrez, J. Cruz, A. Faus-Golfe, J. J. Garcia-Garrigos, D. McCormick, J. Resta Lopez, G. White, M. Woodley, *Optics and Emittance Studies Using the ATF2 Multi-OTR System*, IBIC2012, Tsukuba, Japan, 2012.
- [9] A. Faus-Golfe, J. Navarro, *Emittance reconstruction from measured beam sizes*, to be published
- [10] J. Alabau-Gonzalvo, C. A. Faus-Golfe, J. Resta, R. Apsimon, A. Latina, *Multi-OTR system for Linear Colliders*, IPAC2013 ongoing
- [11] J. Alabau-Gonzalvo, C. Blanch Gutierrez, A. Faus-Golfe , J. Cruz, E. Marin, D. McCormick, J. Resta, G. White, M. Woodley, *Upgrade and Systematic Measurement Campaign of the ATF2 Multi-OTR System*, IPAC2013 ongoing
- [12] J. Giner Navarro, C. A. Faus-Golfe, J. Resta, J. Navarro, J. Fuentes, *Emittance Reconstruction from Measured Beam Sizes* , IPAC2013 ongoing
- [13] *Beam Size and very low-emittance with a muti-OTR system in ATF2*, Thesis J.Alabau



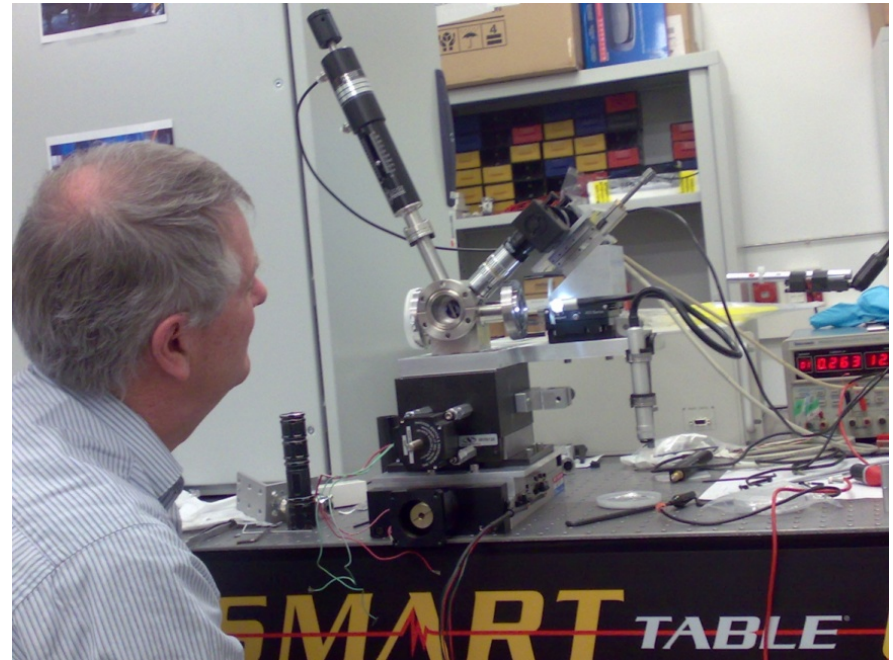
Thanks for your attention



# Back-up Slides

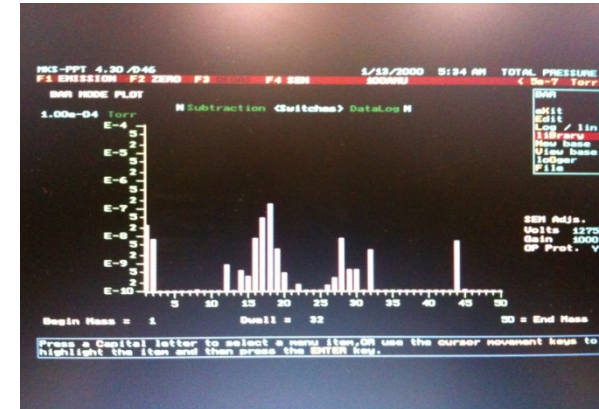
---

# Technical Description HW February 2010: Calibration at IFIC and SLAC



Assembling and first tests at SLAC and IFIC labs after fabrication

Vacuum test made at SLAC

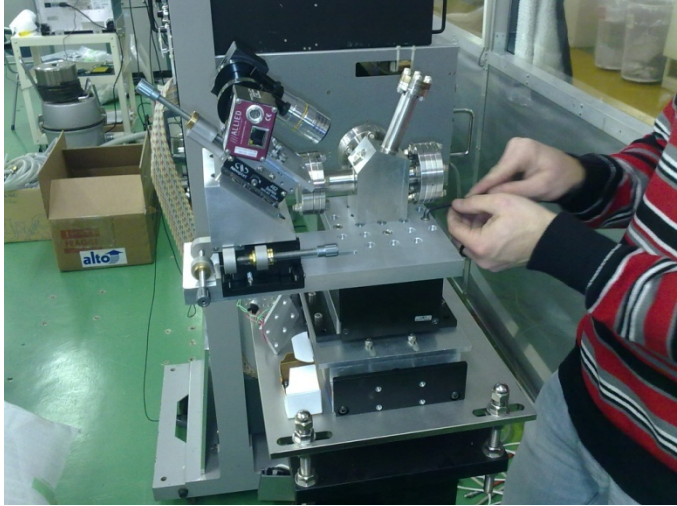


3-4 April

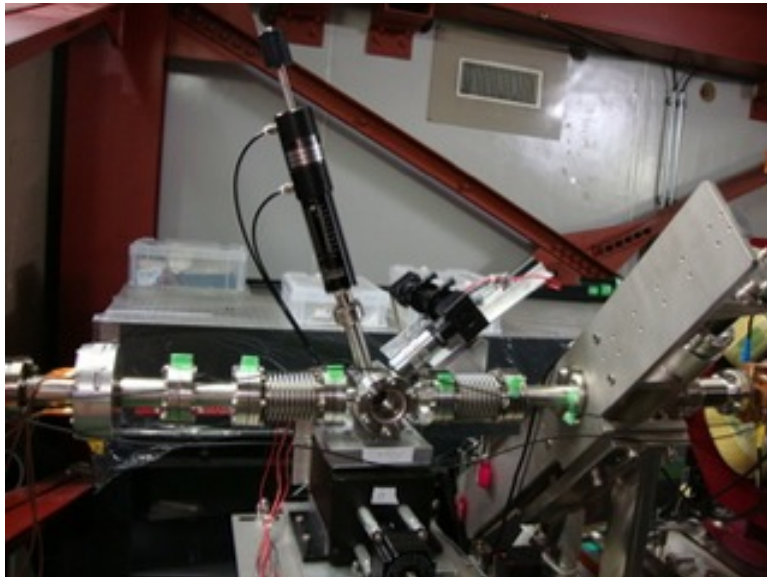
without OTR  
ATF2 Technical Review

with OTR 53

# Technical Description HW April / May 2010: Hardware Installation



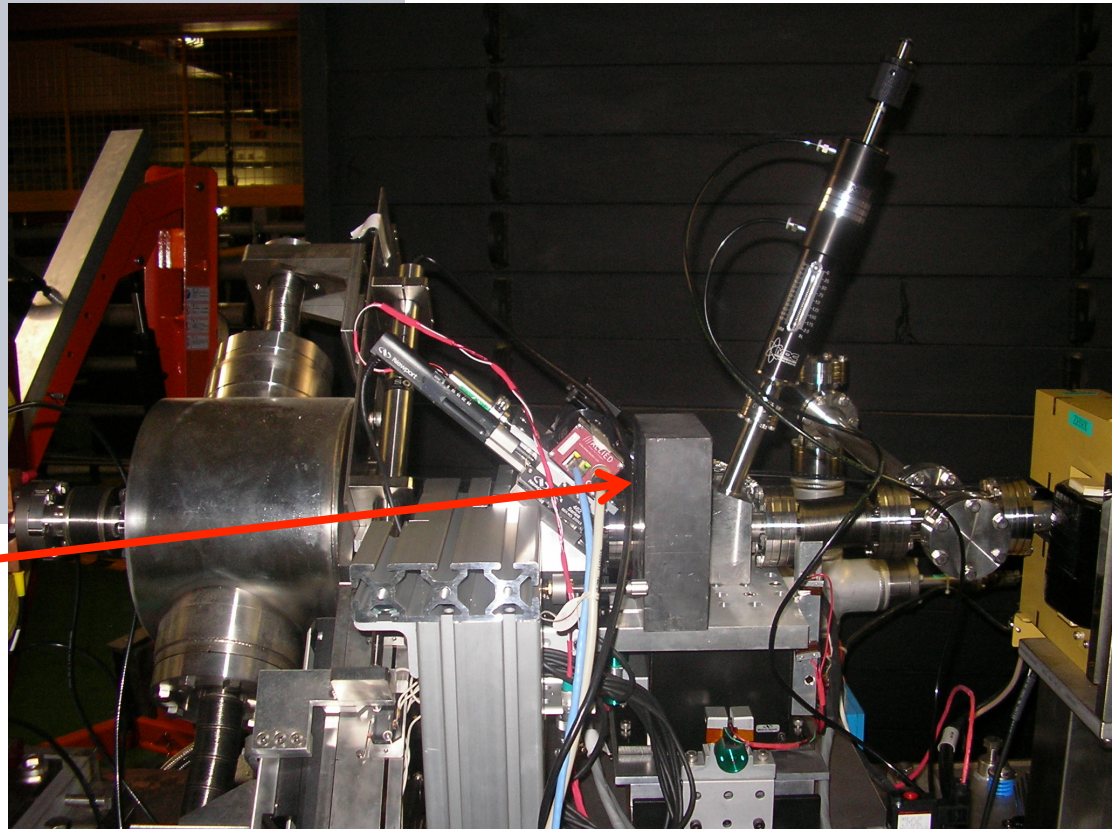
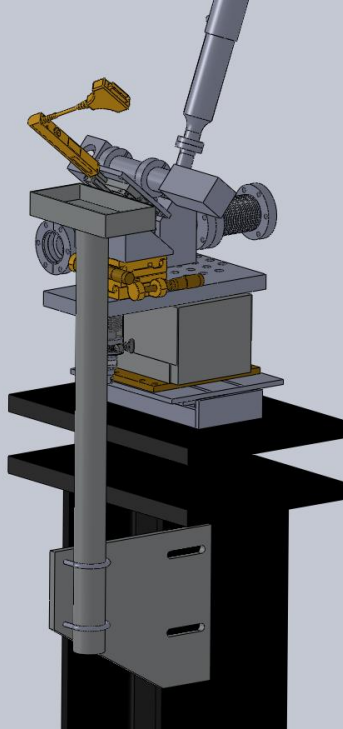
April: All 4 **OTRs** were assembled at ATF clean room



May: All 4 **OTRs** installed in the EXT line

3-4 April

ATF2 Technical Review

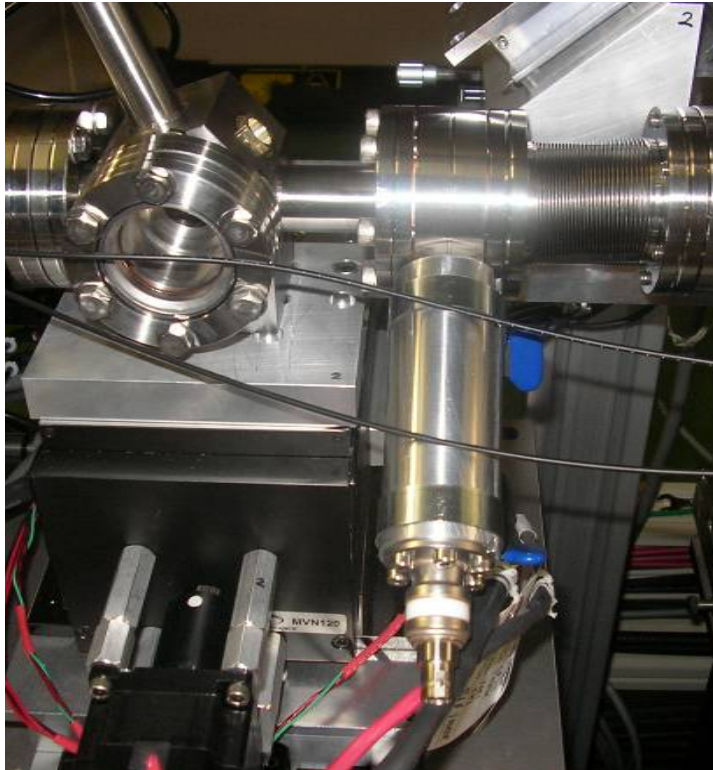


**Lead blocks** with a special holding support has been added to protect cameras from the radiation

3-4 April

ATF2 Technical Review

55



BNC feedthrough, copper connector, ceramic tube with bulb, stainless steel tube (ceramic tube holder), bellow and flange with port.

**Illuminators** were installed to facilitate calibrating tasks by **lighting the target** from the **beam direction**, when there is **no beam**

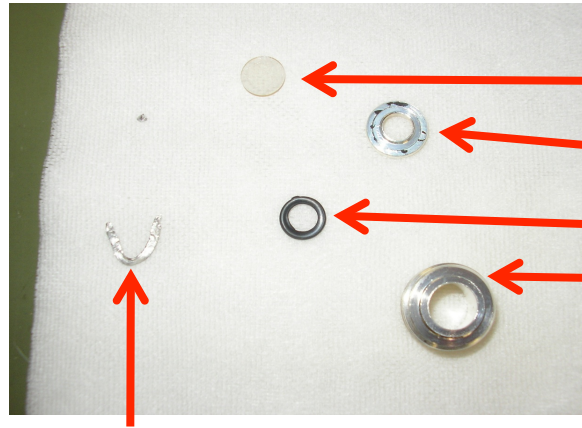
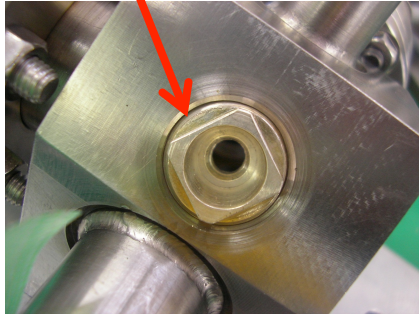


Aluminium tube and clamp to hold the bellow



# Technical Description HW December 2010: Vacuum leak repaired

Leak in the camera window



window

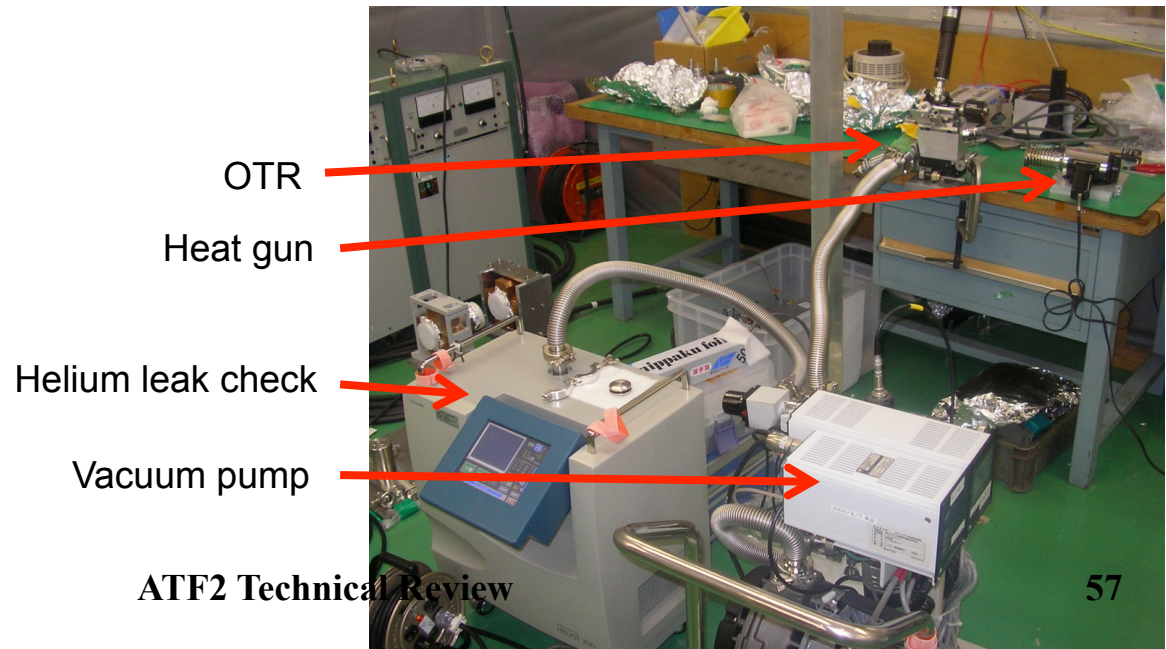
Thrust washer

O-ring

Nut

Old indium washer

Important **vacuum leak** in the camera window of OTR2 was **repaired** by changing the indium washer



OTR

Heat gun

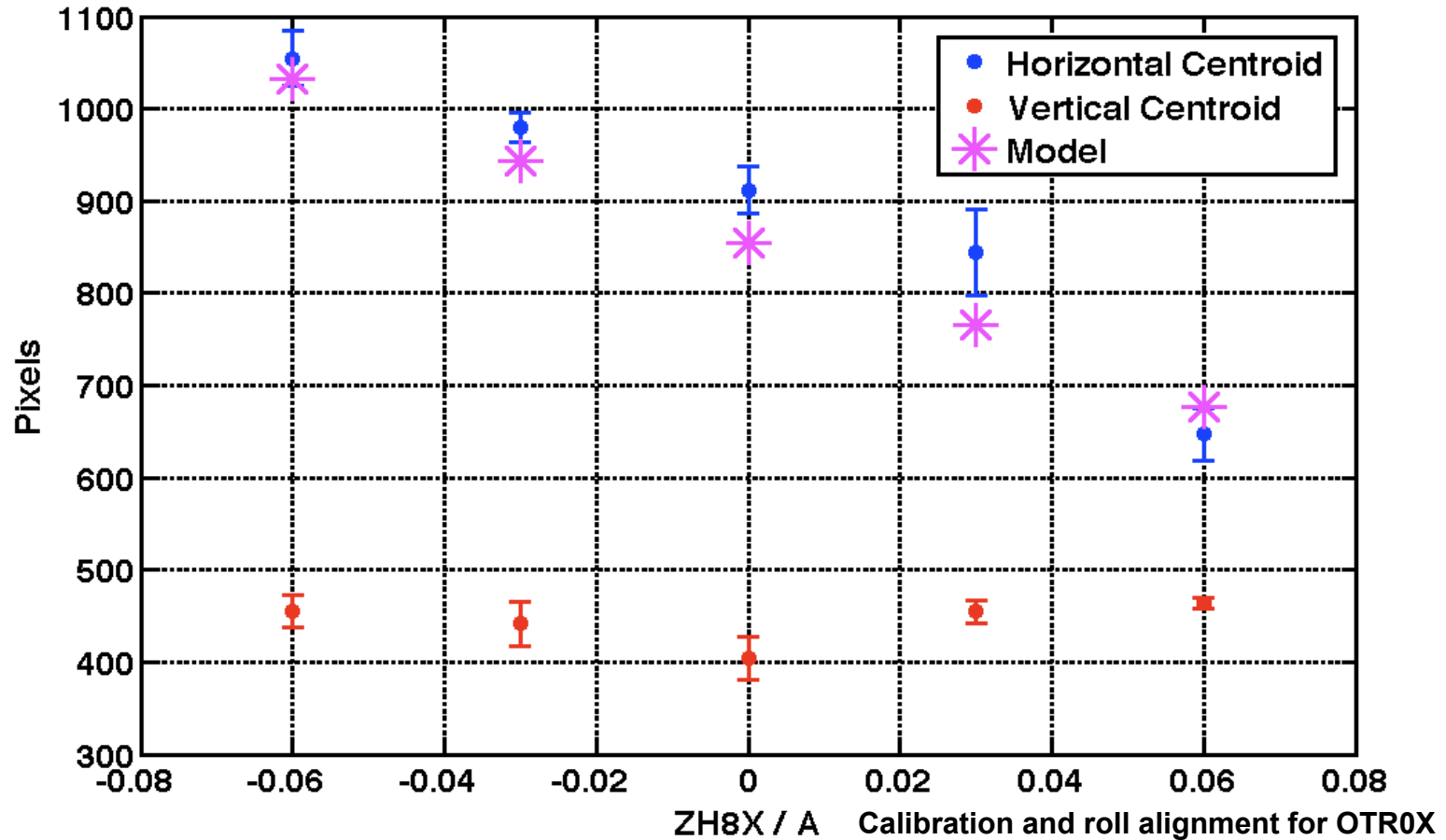
Helium leak check

Vacuum pump

3-4 April

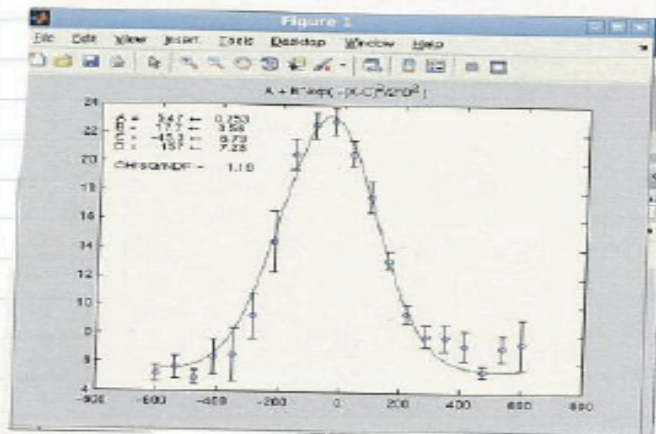
ATF2 Technical Review

57



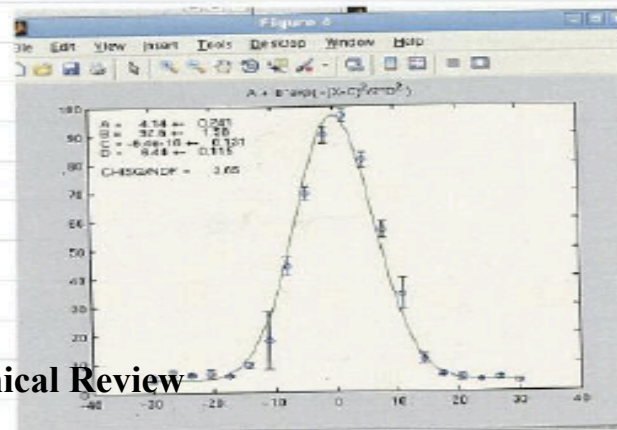
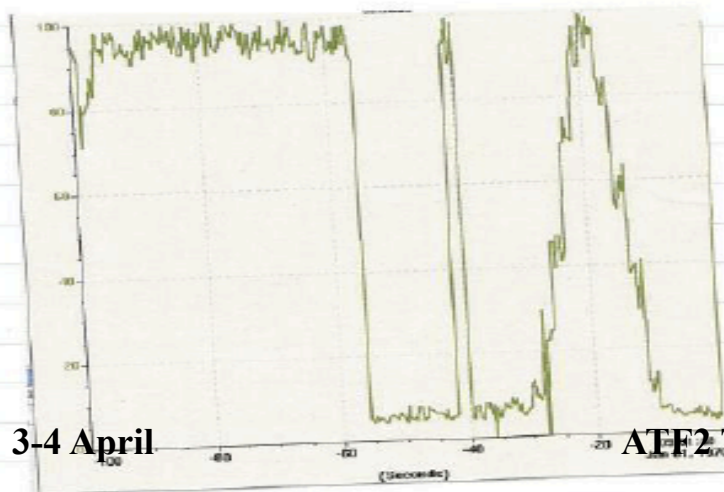
To test the **calibration** an **upstream corrector is scanned** and the response is observed in the OTR. To test **roll alignment (of the OTR CCDs)** we have to look for **no motion in the opposite plane**.

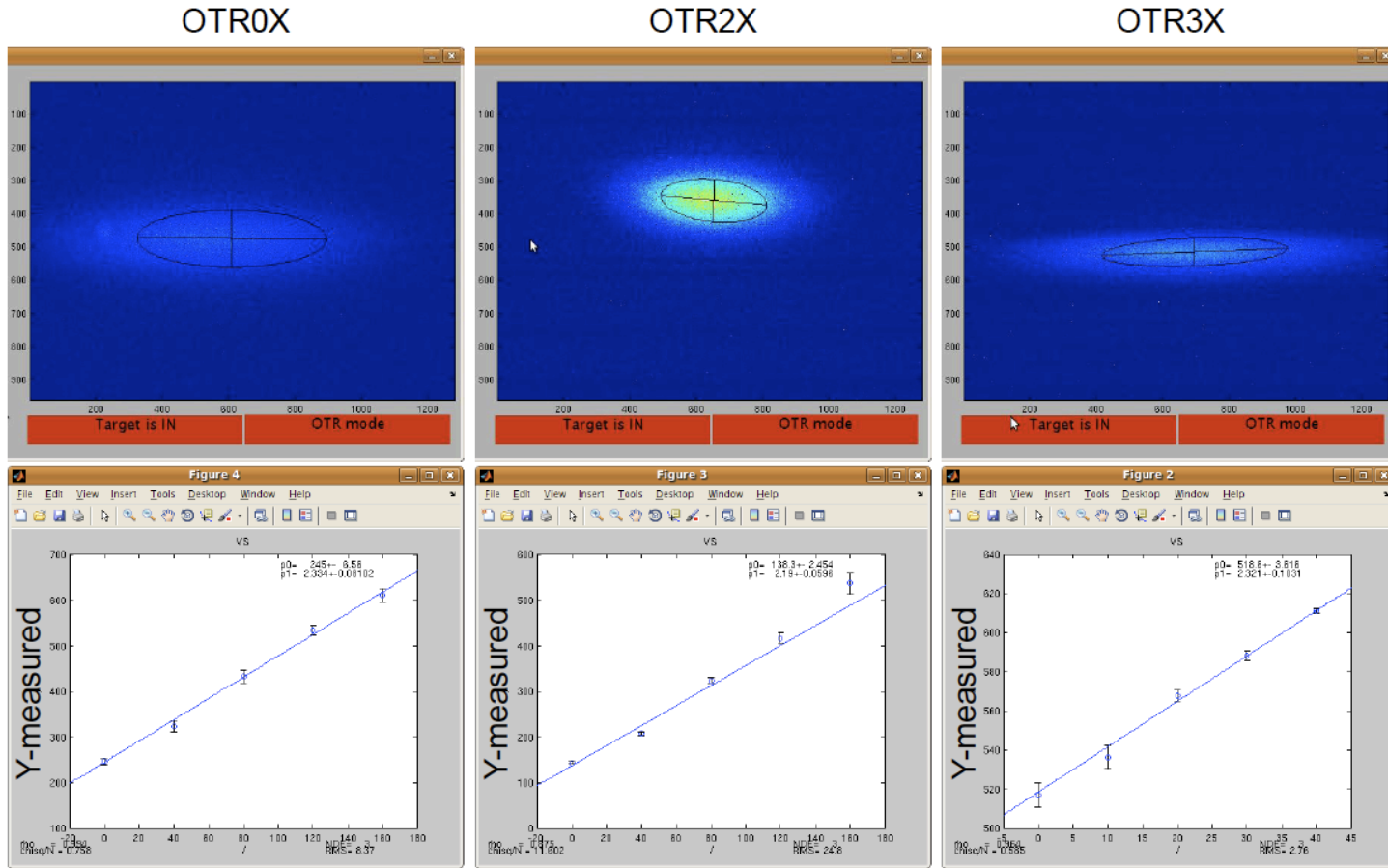
X wire scan from OTR3  
 $\sigma = 157 \pm 7 \mu\text{m}$



**OTR Scan wires** versus signal from **IPBSM background** detector. Made to cross check wire scans with observed beam sizes. Numbers agree within fit errors.

Y wire scan from OTR3  
 BISM signal

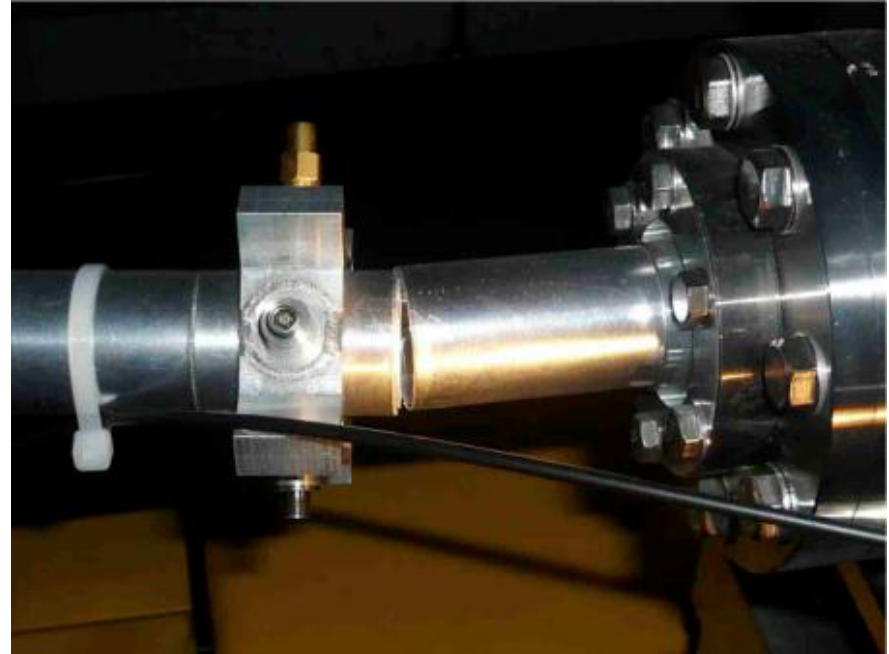




OTR Y-mover Position (μm)

**Vertical scale calibration** done by scanning the vertical mover stage and recording the motion of the observed beam centroid. Thus the vertical calibration factor  $\mu\text{m}/\text{pixel}$  is obtained.

A **LAN controllable power strip in-tunnel** and build in power cycle controls into the OTR software was installed. CCD cameras can be put into a mode of operation unresponsive to the OTR software and needs to be reset by power cycling the cameras being the power supplies in-tunnel.



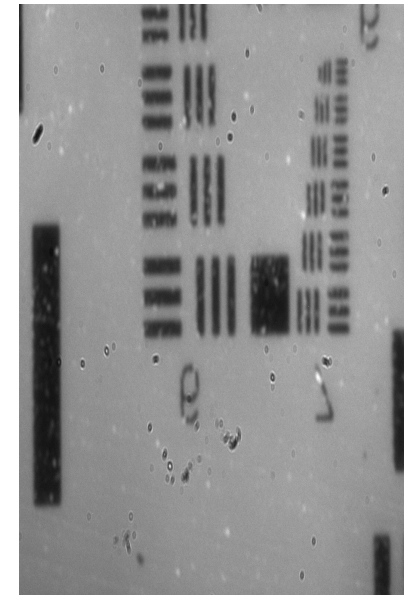
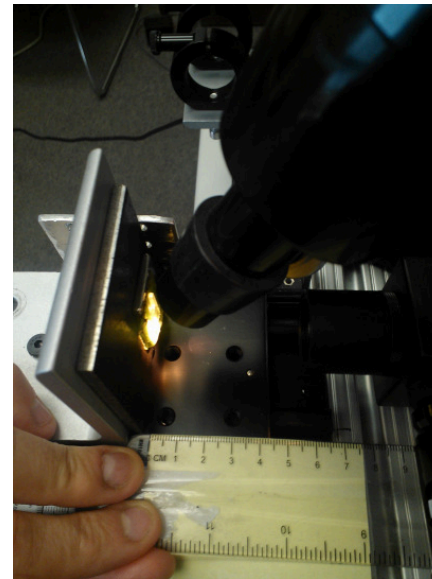
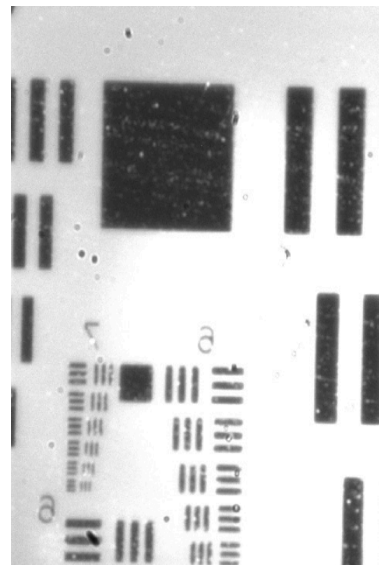
- Impossible to finish the systematic measurement campaign because of the earthquake
- After the earthquake the hardware has been checked and works fine

# Technical Description HW February-December 2012: Design and Construction of new Target holder and Optical system

The present optical device (Mitutoyo lens) implemented by the mOTR system features a working distance of 34 mm and provides a resolution of 10%.

We have designed a new optic device (Achromat lens) that features a working distance of about 55 mm.

To determine the resolution of the new optical system we used an optical bench that accommodates the CCD camera, a tube lens, zoom device, square box with a 45° mirror and the optical system that faces a test target.



Mitutoyo device and CCD image

3-4 April

Achromat new lens and CCD image

ATF2 Technical Review